

<b>REPORT DOCUMENTATION PAGE</b>		Form Approved OMB No. 0704-0188
<p>Public reporting burden for this collection of information is estimated to average 1 hour per response, including the time for reviewing instructions, searching existing data sources, gathering and maintaining the data needed, and completing and reviewing the collection of information. Send comments regarding this burden estimate or any other aspect of this collection of information, including suggestions for reducing this burden, to Washington Headquarters Services, Directorate for Information Operations and Reports, 1215 Jefferson Davis Highway, Suite 1204, Arlington, VA 22202-4302, and the Office of Management and Budget, Paperwork Reduction Project (0704-0188), Washington, DC 20503.</p>		
<b>1. AGENCY USE ONLY (Leave Blank)</b>	<b>2. REPORT DATE</b>	<b>3. REPORT TYPE AND DATES COVERED</b>
	3/18/2004	Final Technical Report, 13 Dec 2002 to 29 June 2003
<b>4. TITLE AND SUBTITLE</b> <b>A02-100: High Gain Antenna for Wireless Local Area Network (LAN), "Multi-Band Coaxial CTS Antenna"</b>		<b>5. FUNDING NUMBERS</b> <b>DAAB32-03-C-0004</b>
<b>6. AUTHOR(S)</b> <b>William W. Milroy, Dr. Magdy Iskander (UofH), and Michael A. Burke</b>		
<b>7. PERFORMING ORGANIZATION NAME(S) AND ADDRESS(ES)</b> <b>ThinKom Solutions, Inc. 3825 Del Amo Blvd., Suite 200 Torrance, CA 90503</b>		<b>8. PERFORMING ORGANIZATION REPORT NUMBER</b> <b>031804-FR01</b>
<b>9. SPONSORING/MONITORING AGENCY NAME(S) AND ADDRESS(ES)</b> <b>US Army CECOM Attn: AMSEL-RD-ST-WL-AA (T. Lu) Ft. Monmouth, NJ 07703-5203</b>		<b>10. SPONSORING/MONITORING AGENCY REPORT NUMBER</b>
<b>11. SUPPLEMENTARY NOTES</b> <b>Prepared with inputs from ThinKom's subcontractor, the University of Hawaii.</b>		
<b>12a. DISTRIBUTION/AVAILABILITY STATEMENT</b> <b>Approved for public release; distribution unlimited.</b>		<b>12b. DISTRIBUTION CODE</b>
<b>13. ABSTRACT (Maximum 200 words)</b> <b>Report developed under Phase I SBIR contract for topic A02-100. US Military mobility and network centric warfare drove need for directive, steerable antennas at 1.8-5.7 GHz. ThinKom (&amp;University of Hawaii) investigated antenna technologies: 1) multi-band coaxial CTS and 2) WAVETRAP, invented by ThinKom. Coaxial CTS and WAVETRAP naturally broad beam, but can generate high gain beams; 20+dB for coaxial CTS and 10+dB for WAVETRAP. For beam steering &amp; sidelobe control, coaxial CTS arrays require phase / amplitude components between radiating elements. WAVETRAP uses simple switching mechanisms to steer and fixed weighting to control sidelobes. Phase I SBIR objective was to span 1.8-5.7 GHz in low profile antenna. Coaxial CTS demonstrated, via UH FDTD analysis, combining of 1.8 &amp; 2.4GHz, and 4.4 &amp; 5.7GHz, but not all four in one array. Four-band coaxial CTS array above PBG ground planes would be 40-50" L X 4" W X 2" H. WAVETRAP spans &lt;1.8-&gt;5.7GHz in one low profile antenna &lt;1" H X 10" D (&gt;gain with &gt; diameter). Coaxial CTS and WAVETRAP offer some of the desired capabilities, however, WAVETRAP's operational simplicity, wide bandwidth and low profile make it ThinKom's choice for development of mobile WLAN commercial products, and therefore the recommendation for military mobile WLAN applications.</b>		
<b>14. SUBJECT TERMS</b> <b>SBIR Report Mobile Wireless LAN Ultra Wide Band Antenna</b>		<b>15. NUMBER OF PAGES</b> <b>39</b>
<b>BEST AVAILABLE COPY</b>		
<b>16. PRICE CODE</b>		

20040806 109

**Low Profile Wideband Antenna  
Multi-Band Coaxial CTS  
Wideband Steerable Antenna/Array**

17. SECURITY CLASSIFICATION OF REPORT	18. SECURITY CLASSIFICATION OF THIS PAGE	19. SECURITY CLASSIFICATION OF ABSTRACT	20. LIMITATION OF ABSTRACT
Unclassified	Unclassified	Unclassified	UL

Standard form 298 (Rev.2-89)  
Prescribed by ANSI Std. Z39-18  
298-102

REF E

**Final Technical Report**  
CLIN 0003  
DAAB32-03-C-0004  
On  
**U.S. Army SBIR Program**  
**A02-100 – High Gain Antenna for Wireless Local Area Network (LAN)**  
**“Multi-Band Coaxial CTS Antenna Array”**  
By  
ThinKom Solutions, Inc.  
ThinKom Report # 031804-FR01  
March 18, 2004

**1. Introduction:**

The US Military's desire for increased mobility and network centric warfare, where the battlefield is interconnected by wireless local area networks supporting broadband data and voice communications, has highlighted the need for more directive and steerable antennas capable of operating across several bands (roughly 1.8 to 6 GHz). In response to this need ThinKom proposed to investigate two alternative promising alternative antenna technologies: 1) multi-band coaxial CTS and 2) WAVETRAP, a wideband antenna technology newly invented by ThinKom. Since the inventor of Coaxial CTS, Dr. Iskander, is presently a professor at the University of Hawaii, ThinKom subcontracted to Dr Iskander's research team for that portion of the conceptual design and evaluation of the multi-band coaxial CTS array alternatives. In parallel ThinKom itself performed the conceptual design and evaluation of the wideband WAVETRAP alternative.

Both coaxial CTS and WAVETRAP are naturally broad beam (near omni-directional) antenna technologies, however, it is thought that by arraying multiple coaxial CTS elements together within a single antenna structure that a more directive beam with higher gain in the azimuth plane could be achieved. As it turns out, the WAVETRAP antenna technology also appears to have the capability of forming a more directive beam in the azimuth plane by independently feeding individual azimuth segments of the WAVETRAP antenna structure, possibly not as directive as may be achieved by arraying a large number of coaxial CTS elements. To be useful, these directive beams must be steerable in the azimuth plane and have some degree of sidelobe control or sidelobe reduction. To achieve this control for the coaxial CTS array will require that phase and amplitude control elements will need to be inserted between the individual elements and individually controlled by some form of control feed or bus. In the case of the WAVETRAP approach a simple switching mechanism is used to steer the beam and a simple fixed weighting scheme used to reduce sidelobes. While these are significant issues to be considered in choosing the final configuration, they were not investigated during this Phase I project. The key issues addressed were the fundamental ability to cover (span) the desired frequency bands and the low profile nature of the resultant antenna architecture.

The desired operating bands (to maximize commercial synergy with this proposed military mobile wireless networks) are 1.8-2GHz, 2.4-2.5GHz, 4.4-4.5GHz & 5.7-5.9GHz. The coaxial CTS approach was to first demonstrate individual arrays spanning each of the individual bands, and then to combine those individual elements and arrays together into a multi-band array. The UH team was able to demonstrate, via FDTD analysis, combining of the 1.8 & 2.4GHz bands, the 4.4 & 5.7GHz bands, and the 2.4 & 5GHz, however, they never combined all four bands into a single array. At the same time the UH team also investigated the use of photonic band-gap ground plane technology to provide a broad band ground plane over which to mount the coaxial CTS array to help minimize (roughly by X2 for half high element above the PBG ground plane) the overall height of the coaxial CTS array (note that the individual coaxial CTS element vary in diameter based on their operating frequency; the lower the frequency, the larger the diameter or height – for example for the lowest band, 1.8GHz, the diameter would be about 3.5inches or just under 2inches high when a half diameter is mounted above a PBG ground plane). Overall the size and height of the coaxial CTS could be fairly large, assuming all four bands could be achieved by arraying the four different elements (multiples of each as needed to achieve the desired gain), and mounting the entire assembly above one or more PBG ground planes.

In contrast to the coaxial CTS approach, the WAVETRAP would be designed to span the entire desired commercial operating band (1.8 to 5.7GHz) in a single low profile structure of less than 1 inch in thickness and about 10 inches in diameter. Increasing the diameter of WAVETRAP will increase the gain both for the broad beam and the directive modes.

In summary, while both coaxial CTS and WAVETRAP appear to offer capabilities (at least potential capabilities), the simplicity of operation, wide operating bandwidth and very low profile (& small size) of WAVETRAP make it the choice by ThinKom for continued development of mobile WLAN commercial products and therefore the preferred choice for military mobile WLAN applications.

## **2. Identification and Significance of the Problem or Opportunity:**

The US Military increasingly is making use of commercial products and systems, especially communication systems, such as wireless local area networks (WLANs) and personal communication systems (PCS). The Military needs high data rates as well as voice communications, and needs to be able to set up and maintain these local area communication networks in remote locations where no infrastructure exists. In addition, the Military needs security and ruggedness as well as the ability to operate in various terrains and environments. Further, the network needs to be able to move with the troops, vehicles and aircraft that form the communication nodes of the network. Even more, the network needs to operate when the nodes are all moving relative to each other, and some of the nodes may be entering and/or leaving the network. The varying terrain and environments, and the constant motion of the nodes in the network present some especially difficult challenges for the antennas associated with each of these nodes. These difficult environments present a severe and ever changing interference situation for these antennas to operate in. Because of the constant motion and nodes entering and

leaving the area of the WLAN, the node antennas must have broad angular coverage (near omni-directional), but because of the ever-changing interference environment, the antennas must also be able to reject this interference and must be able to enhance the communication link(s) with other network nodes. Under some circumstances it may even be desirable to emphasize the communication with another specific nodes, and therefore to significantly enhance the communication link with that specific node. To increase the communication link, the node antenna must be able to selectively increase the antenna gain in the direction of the desired node. But since these nodes are all in constant motion, then the antenna must be capable of dynamically changing this gain and the specific direction of said increased gain. That suggests a phased array antenna, but this antenna must be small in size (aperture extent), light-weight and low profile (to not put a burden on the platform or foot solder carrying the node), and must be affordable so that nearly all vehicles and solders can be equipped with said nodes. Presently such antenna arrays are not small, light, low profile or low cost (especially not low cost), but the promise of coaxial CTS and recently developed ferroelectric devices and phase shifters suggest that such array antennas might be feasible. However, to take full advantage of those WLAN commercial communication products, these antenna arrays must also be able to operate across a number of frequency bands, such as the PCS band (1850-1990 MHz) and WLAN bands (2.4-2.5 GHz, 4.4-4.5GHz and 5.7-5.9GHz).

### **3. Statement of Proposed Solutions:**

#### **Phase I Technical Objectives**

Trade off and select either a broadband (capable of being tuned from 1.8 to 6 GHz) or stacked multi-band (capable of supporting multiple [at least two] sub-bands within the 1.8 to 6 GHz range) version of coaxial continuous transverse stub (CTS) antenna technology. The selected antenna element will be arrayed (initially a 1X4 array prototype for Phase II evaluation) over a wideband photonic bandgap (PBG) ground plane providing consistent performance across the 1.8 to 6 GHz frequency range, and controlled by ferroelectric devices and phase shifters to select the operating band, and/or shape and steer the beam across at least a +/- 90 degree angular range. Making use of these components and features (selected with customer concurrence), design and project antenna performance and concept feasibility using electromagnetic modeling, such a wideband or multi-band array. These high gain antenna designs should optimize operation in the following bands: 1850-1990 MHz, 2.4-2.5 GHz, 4.4-4.5 GHz and 5.7-5.9 GHz. The resulting array prototype is intended for fabrication and evaluation during Phase II to demonstrate the feasibility and performance capability of a high data rate, dynamic Wireless Local Area Network (WLAN) set up and maintained amongst a number of mobile (such as air and ground vehicles) nodes which may be in constant motion and/or which may periodically enter and/or leave the network.

## Phase I Work Plan

### Introduction

Planar Continuous Transverse Stub (CTS) was originally invented at Hughes Aircraft Company in 1991. It represents a unique class of low-cost antenna array, exploiting the low-loss, low-dispersion, dimensional robustness, and design flexibility of an open parallel-plate structure as both its transmission line and radiator bases. The coaxial CTS array, however, provides an alternative design that may provide additional advantages in feeding, impedance matching, and radiation characteristics. It consists of a coaxial structure as its transmission line feed and parallel plate subs as the radiating elements. The difference between the coaxial CTS and the planar version is their array structure in the form of annular or sectoral stubs and the resulting omni-directional radiation pattern. As in the case of planar CTS, beam steering may be achieved mechanically or by using Ferroelectric materials.

### Coaxial CTS Design

Fig. 3-1 shows a two-element coaxial stub CTS antenna array, where it may be seen that it consists of a cascaded section of standard coaxial transmission lines and open-ended coaxial radiating stubs. Similar to the planar CTS case, short-circuited stubs may also be used and the coaxial CTS arrangement may be used as a filter in this case. Design procedures for a coaxial CTS array include the determination of the following parameters: (1) width of stub segment L1; (2) length of transmission line segment L2; (3) dielectric constant of filler dielectric material  $\epsilon_r$ ; (4) diameter of inner conductor D1; (5) diameter of outer conductor D2; and (6) diameter of stub D3.

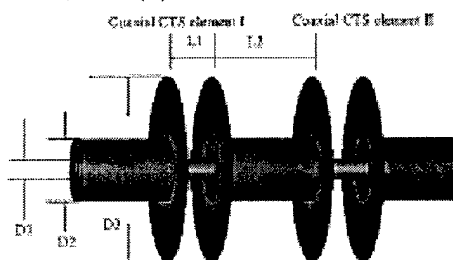


Figure 3-1. Coaxial CTS array segment with two elements.

For the purpose of an illustrative design, the width of stub segment L1 was selected to be a half wavelength in dielectric material that fills the stub. The length of the transmission line segment L2 and dielectric constant of dielectric material  $\epsilon_r$  can be chosen to fulfill distance and phase demands between stubs.

The diameters of the inner and outer conductors D1 and D2 of the coaxial transmission line can be adjusted to form the desired value of impedance, such as 50 or 75 in the case of a coaxial transmission line. The ratio between and determines the radiation pattern, voltage across, and the radiated power from each stub. Small values of D3/D2 tend to lead to increased radiation, but more care must be taken to achieve impedance matching.

Also, D<sub>3</sub> must be chosen so as to limit the level of mutual coupling between the stub elements in the Coaxial CTS array. Control of mutual coupling between elements in the array can be generally achieved by meeting the condition D<sub>3</sub>>L<sub>1</sub>.

The diameters of the inner and outer conductors D<sub>1</sub> and D<sub>2</sub> do not need to be uniform along the transmission line. Instead, they can be changed periodically to adjust the matching and phase relationship between elements. Actually, coaxial CTS is an excellent self-matching structure. By properly controlling the ratio of D<sub>3</sub> and D<sub>2</sub> and the ratio of D<sub>3</sub> and L<sub>1</sub>, it is possible to achieve low reflection stub elements. As one might expect, the design parameters D<sub>2</sub>, D<sub>3</sub>, L<sub>1</sub>, and L<sub>2</sub> impact various aspects of the characteristics of the array including impedance matching ( $S_{11}$ ), percentage of power radiated out, and radiation pattern. Detailed design curves will be developed and reported in a separate publication.

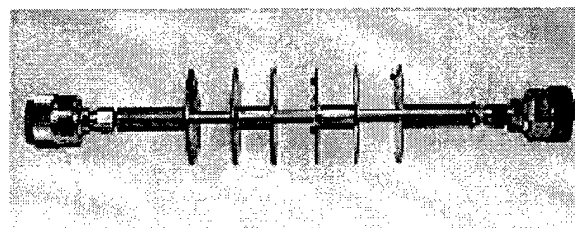


**Figure 3-2.** Photograph of the prototype X-band three-element Coaxial CTS array.

### Multi-band Coaxial CTS antenna Array

The next step was development of a multi-band coaxial CTS antenna array. For the multi-band design, it was desired to have two sets of stubs: one that was non-radiating (full transmission) at lower frequencies and radiate effectively at higher frequencies (high frequency stubs), and a second set of stubs that radiate at the lower frequency (low frequency stubs). The two sets need to be arranged in tandem with the high frequency stubs near the input. This way, high frequency signals would radiate from the high frequency stubs before reaching the low-frequency stubs at the end, and the low frequency signal would efficiently pass through the high frequency stubs and radiate most (if not all) of the signal when reaching the low frequency stubs at the end of the array.

To accomplish this, it was necessary to know the electrical dimensions that would produce full transmission for the high frequency stubs at the lower frequency. For this purpose, structures with narrow gaps and long stub diameters were simulated. It was found that narrow gap ( $\ll \lambda$ ) stubs with a stub diameter of approximately  $\lambda/3$  (12 mm at 8 GHz) or longer will produce close to full transmission at the lower frequencies. At higher frequencies, however, the same physical dimensions of the stubs were found to radiate efficiently. It is therefore possible to design a coaxial CTS structure that produces efficient radiation at a high frequency and appears almost transparent at lower frequencies.

Using this approach, we simulated a coaxial CTS array with multi-band performance. This multi-band array was designed with the structure possessing two sets of three stubs each. The first three stubs were designed to radiate at high frequencies and be non-radiating (close to full transmission) at low frequencies. The second set of stubs was designed to radiate at low frequencies.

The multi-band array was designed at 4.2 GHz (C-band) and 19.4GHz (K-band). This upper frequency was chosen to provide a good test of the accuracy of our model, as well as to test the dimensional sensitivity at the higher frequency.

The design was dielectrically loaded with Teflon and polyethylene to help improve impedance matching and reduce the size of the array. Further performance enhancements were achieved using control of the stub gap, stub height, and stub spacing of both high and low frequency stubs.

After initial simulations, it was clear that we needed to simulate the entire six-element structure simultaneously and as one unit. Due to mutual coupling effects, it was difficult to achieve single frequency performance that would not be altered when the two arrays of stubs were cascaded.

Following a manual optimization using in-house FDTD codes, a multi-band coaxial CTS antenna array design was achieved that produced low reflection and good radiation characteristics at both the upper and lower frequency bands. The dimensions of the high frequency stubs were  $L_1 = 5.2$  mm,  $L_2 = 3.8$  mm,  $D_1 = 1.12$  mm,  $D_2 = 3.6$  mm, and  $D_3 = 44.4$  mm. The dimensions of the low frequency stubs were  $L_1 = 18.9$  mm,  $L_2 = 29.6$  mm,  $D_1 = 1.12$  mm,  $D_2 = 3.6$  mm, and  $D_3 = 61.2$  mm. The spacing between the last high frequency stub and the first low frequency stub in the tandem connection of the two arrays was 21.6 mm. The radial waveguide stubs were dielectrically loaded with Teflon rings. The coaxial line of the multi-band array was filled with polyethylene. The Teflon (stubs) and polyethylene (coaxial line) were both simulated with  $\epsilon_r = 2.2$  and  $\tan \delta \sim 0$  (negligible dielectric losses). Fig.3-4 shows a schematic of the designed multi-band six-element array, and Fig. 3-5 shows a photograph of the fabricated and tested array.

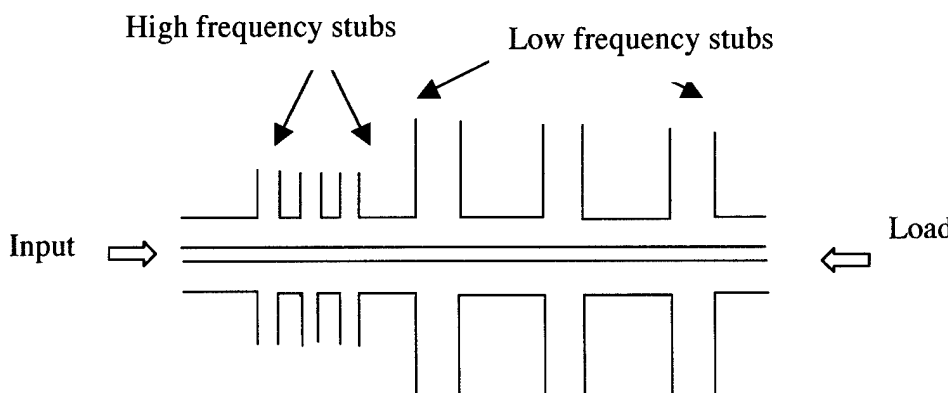


**Figure 3-4.** Axial view of six-element multi-band coaxial CTS antenna array. First set of stubs from input are high frequency stubs. Second set of stubs from input are low frequency stubs.

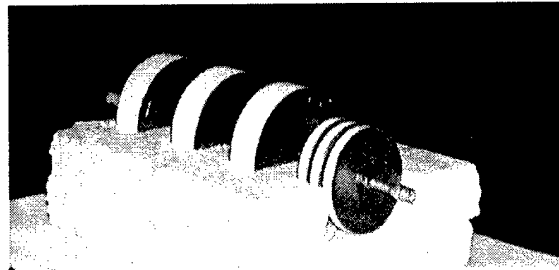


**Figure. 3-5.** Photograph of fabricated multi-band six-element coaxial CTS antenna array designed to operate at 4.2 and 19.4 GHz: Angled View.

Following fabrication of the six-element multi-band coaxial CTS antenna array, the physical dimensions of the structure were measured and found to be in accord with the design parameters. There was a slight air gap between the machined Teflon rings and the polyethylene-filled coaxial transmission line at the base of the stub. A new FDTD model was constructed that matched these measured physical dimensions and included the deviations from the initial design. Simulations were then run on this new model to allow for comparison with the measured S-parameters and radiation patterns.

### **WAVETRAP – Ultra-Wideband, Low-Profile Antenna**

In addition, we plan to use ThinKom's WAVETRAP antenna product, being developed for commercial multi-band WLAN applications, to compare against the proposed coaxial CTS array antenna to determine what enhanced performance and operational capabilities can be added as beam control features of the array.

ThinKom's WAVETRAP antenna technology represents a commercially viable and an effective solution for achieving multi-octave bandwidth, multi-functionality, and high efficiency in a single compact antenna element. These features are achieved by utilizing a novel internal electromagnetic architecture that is passive, simple, and low-cost, yet allows sufficient degrees of freedom to customize both its pattern and bandwidth properties. Design attributes including antenna size, operating bandwidth, efficiency, directivity, and beamshape(s) can therefore be traded in order to provide optimized solutions for specific applications. The WAVETRAP antenna is ultimately capable of simultaneously supporting both "omni-directional" (fixed hemispherical) and "directive" (steerable lobes and/or nulls) beams via multiple (coax) feed ports.

The mechanically-robust antenna design is comprised of a small number of individual subassemblies, fabricated utilizing low-cost commercially-available materials (structural plastics) and processes (injection-molding and electro-less plating) and assembled in a low-cost, low-precision "snap-together" fashion. This plastic construction assures low-cost (commercial-viability) and light weight as well as adding the fabrication flexibility required to support both planar and curved installations.

The "Basic" or "Dominant Mode" version of the antenna element supports a quasi-omni-directional, phi-symmetric antenna pattern (similar to a monopole). The dominant mode

in this particular case is launched via a coaxial interface at the center-rear of the antenna. “Directive” or “Multi-Mode” versions of the antenna element support azimuth beam-forming functions in which one or more defined lobes and/or nulls can be adaptively “pointed” in the azimuth direction. In this case, the requisite mode set within the structure is launched via a number of equally-spaced coaxial feed points located along a circular pattern on the rear of the antenna. It is anticipated that directive peak gains of +10 dBi and null-depths of -20 dBi will be achievable using this approach. Note that the radius of this circle and the spacing of the elements for the “Multi-Mode” version of the antenna are chosen such that both the omni-directional and directive functions can be simultaneously and independently supported, at the same or different operating frequencies.

In addition to a reconfigurable azimuth beam shape flexibility, the elevation beamshape of the antenna, as a function of frequency, can be customized in order to provide increased directivity in either the zenith/nadir-oriented or horizon-oriented directions. As an example, this design feature can be exploited in wideband communication applications, where terrestrial sources (horizon) are favored in one frequency range while satellite sources (zenith or omni) are favored in another frequency range.

Logarithmically-spaced Annular “stubs” of varying widths form the actual radiating surface. By restricting the maximum width of these stubs to values less than one-half wavelength at the highest operating frequency, we can accurately treat (to first-order) each annular ring as a filamentary circular magnetic current source, computing its pattern characteristics directly in terms of its associated Electric Vector Potential. This collection of ring sources therefore closely mimic the equivalent surface-currents associated with a “standard” monopole over a ground-plane. However, unlike a monopole, this antenna implementation can support multiple octaves of frequency bandwidth without the formation of nulls and while maintaining a quasi-constant input match (high efficiency). To achieve this unique capability, the widths and radii of the radiating stubs and the geometry of the internal radial waveguide-sections are chosen such that an effective (but compact) multi-stage impedance transformer is formed by the ensemble. In this way the impedance “seen” by the coaxial interface at the center of the array is adequately maintained at or near the desired 50 ohm value. Figure 3-6 illustrates the predicted antenna patterns for the basic “omni” version of the antenna, comprised of 4 annular rings, over the frequency range of 0.50 to 6.00 GHz.

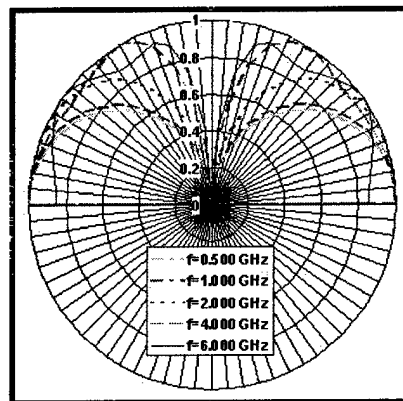


**Figure 3-6.** Predicted Antenna Patterns for “Basic” Element

A prototype of this antenna, approximately 6 inches in diameter and 1 inch in depth is currently under development (internally funded). This initial prototype will demonstrate a minimum efficiency of 70%, providing null-free omni-directional coverage and a minimum gain of between +1 and +4 dBi over the continuous frequency range of at least 2 GHz to 6 GHz. Subsequent prototypes will demonstrate the selectable directive beam capability and an ability to simultaneously operate in several separate sub-bands, but with modest isolation between those sub-bands.

#### **4. Investigations and Results Thereof:**

##### **4.1 Multi-Band Coaxial CTS Antenna**

The students and staff of the Hawaii Center for Advanced Communications under the direction of Professor Magdy Iskander, College of Engineering, University of Hawaii at Manoa (UH) have been acting as consultants to ThinKom for the multi-band coaxial CTS array design, simulation and analysis feasibility effort during the early portion of this Phase I contract. By building upon the previous coaxial CTS (UH holds a patent on the coaxial CTS technology and ThinKom has a license to the other CTS patents held by Raytheon) development efforts at other frequency bands (see Figure 4.1-1), the RF design team first designed and analyzed individual coaxial CTS arrays for each of the customer defined wireless LAN bands of interest: 1.8-1.99 GHz, 2.4-2.5 GHz, 4.4-4.5 GHz, and 5.7-5.9 GHz. Also see Figure 4.1-2 for a brief explanation of the theory of operation of the multi-band coaxial CTS array.

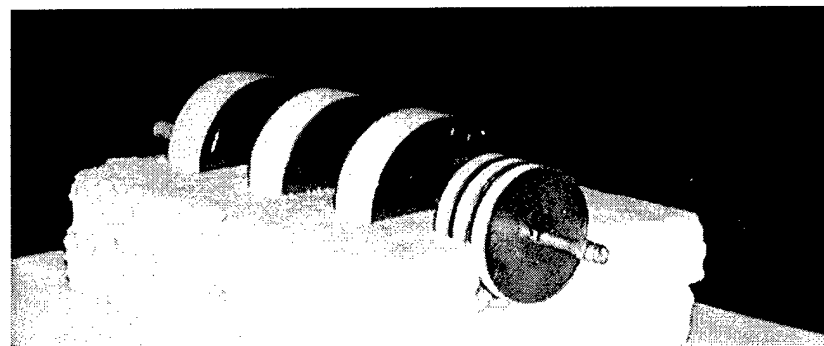
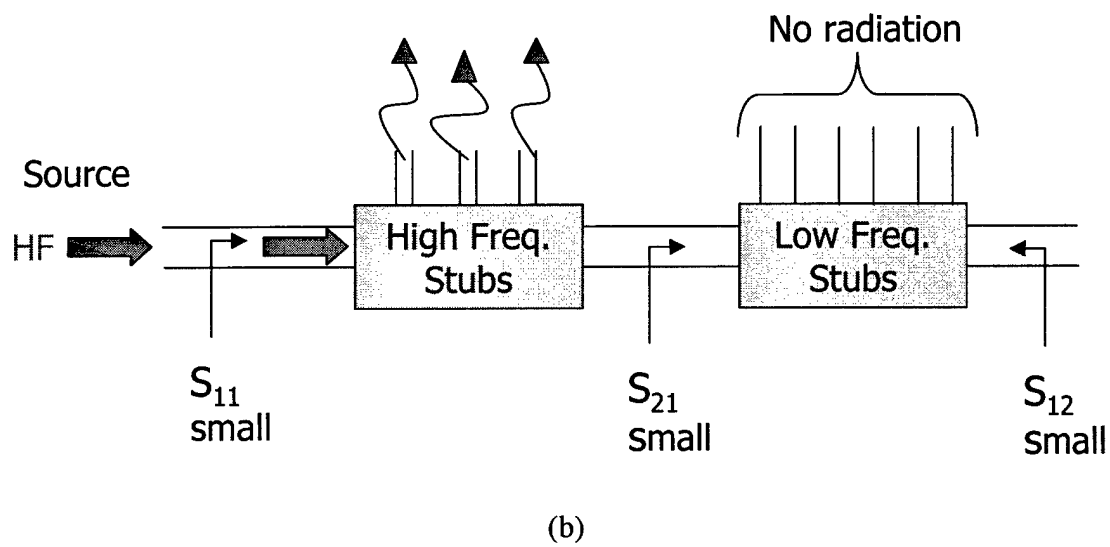
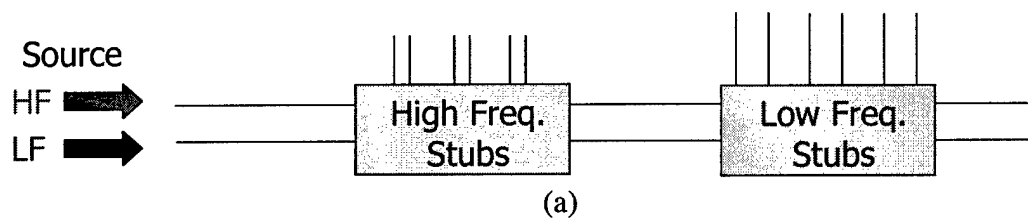
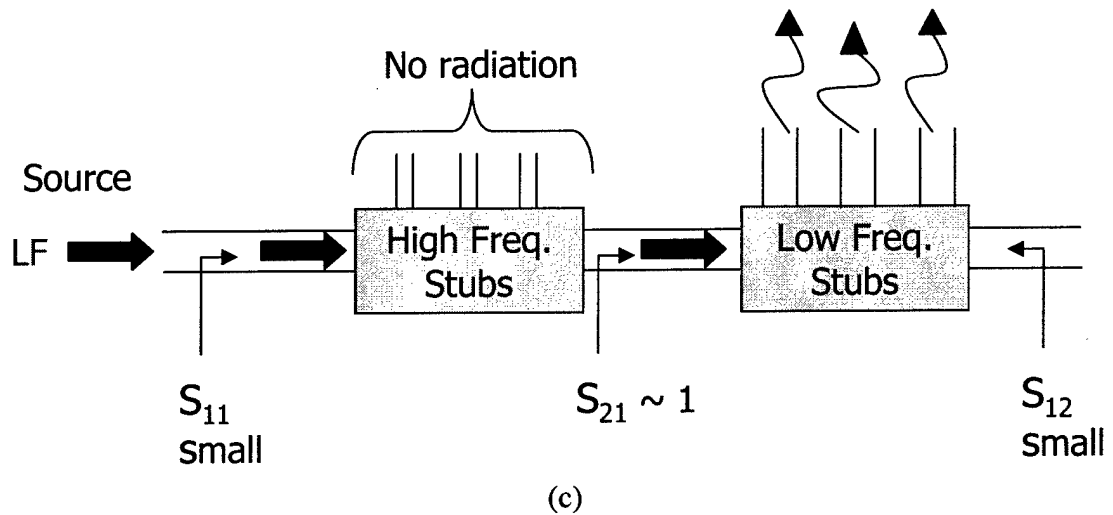


Figure 4.1-1. Picture of Existing Dual Band Coaxial CTS Arrays

## High frequency and Low frequency stubs.





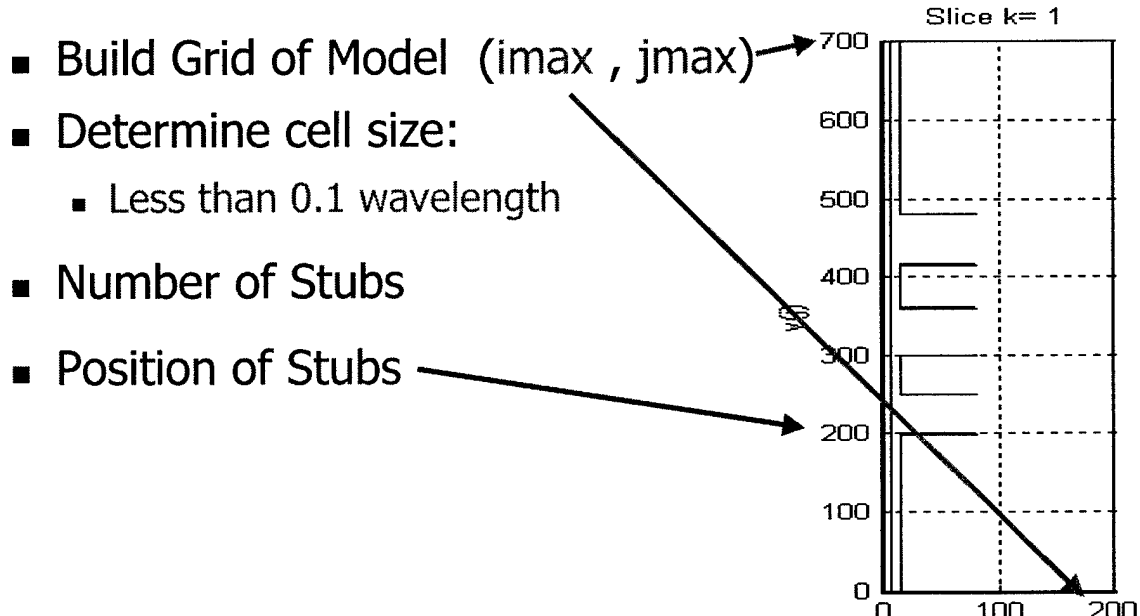
**Figure 4.1-2.** Theory of Operation of Dual Band Coaxial CTS Arrays,

(a) Both High and Low Frequency Stubs as shown in Fig 4.1-1

(b) High Frequency Coupled only into High Frequency Stubs

(c) Low Frequency Coupled only into Low Frequency Stubs

Dr Iskander's UH team developed in-house analysis tools based on FDTD techniques to help in the analysis and synthesis of various coaxial CTS architectures, including multi-band arrays. Figure 4.1-3 outlines how the physical elements of a particular coaxial CTS array design are captured in this analytical tool and subsequently used to estimate operating performance of resultant antenna, as shown in Figure 4.1-4. In Figure 4.1-5 a previously designed, built and tested single band coaxial CTS array is duplicated using FDTD techniques and the FDTD estimated performance compares well against the previously measured test results. Similarly, in Figure 4.1-6 a previously designed, built and tested multi-band coaxial CTS array is compared favorably against the FDTD model thereof.



- Sections of Coax
- Inner Radius and Outer Radius of Coax
- Stub Radius
- Stub Gap
- Stub Spacing

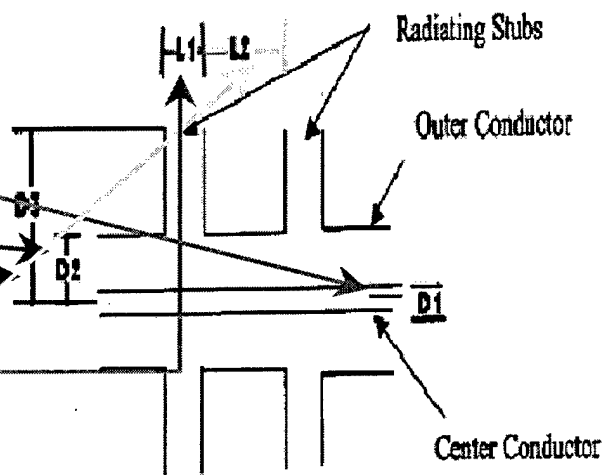
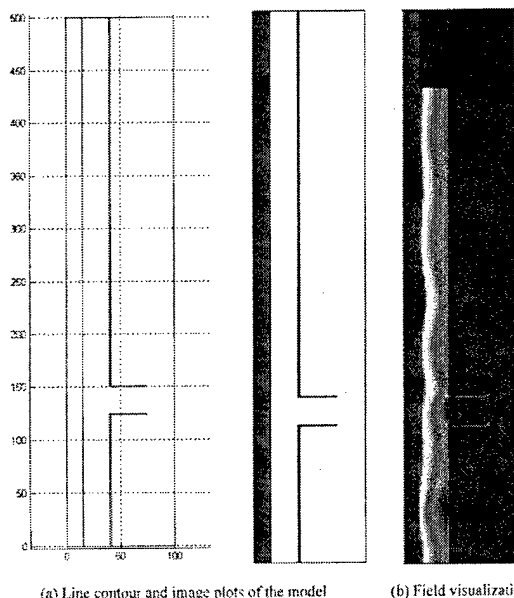


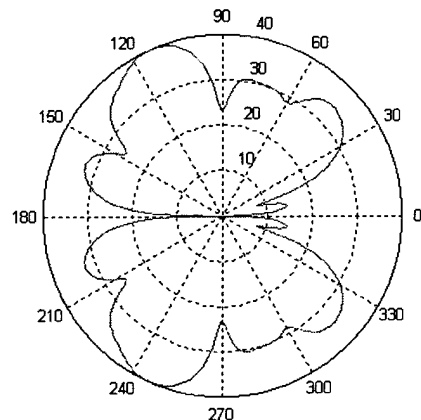
**Figure 4.1-3.** Building FDTD Model of Coaxial CTS Array



- Matlab is used to visualize the output
- Line contour plot shows model of antenna
- Field visualization of the E-field in the coax/stub and outside antenna

(a) Line contour and image plots of the model      (b) Field visualization

Fig. 2. Model and field visualization



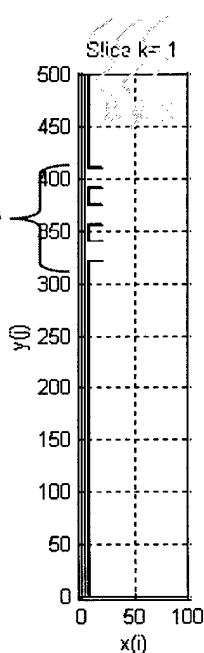
- Radiation pattern
  - Mirror image from  $180^\circ - 360^\circ$
- $S_{11}$  and  $S_{12}$

$$S_{11} = 0.29193 \quad S_{12} = 0.25751$$

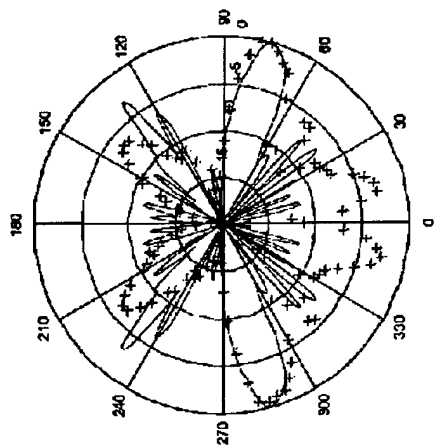
$$S_{11} = -10.7 \text{ dB} \quad S_{12} = -11.78 \text{ dB}$$

**Figure 4.1-4.** FDTD Model Outputs for Coaxial CTS Array

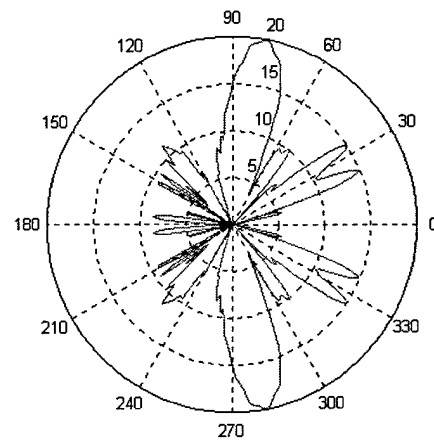
- 3-element array
- Stub Parameters:
  - Radius: 20 mm
  - Width of gap: 18.75 mm
- Positions:
  - Stub 1: 340 mm
  - Stub 2: 375 mm
  - Stub 3: 410 mm



- Coax Parameters:
  - Inner radius: 3 mm
  - Outer radius: 6.9 mm
- Cell Size Used: 1 mm  
(scale is in cells)



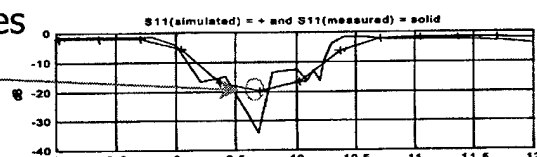
Previously simulated radiation pattern.



Our simulated radiation pattern.

- Previously Simulated Values

- $S_{11} \sim -20 \text{ dB}$
- $S_{12} \sim -10 \text{ dB}$



- Our Simulated Values

- $S_{11} = -21 \text{ dB}$
- $S_{12} = -12.1 \text{ dB}$

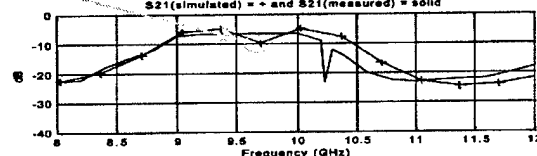


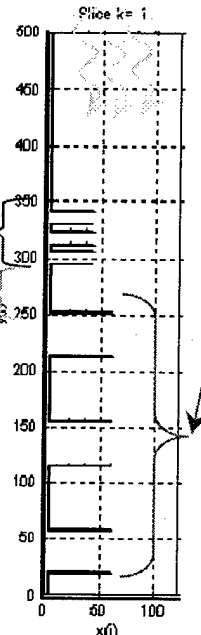
**Figure 4.1-5.** Previous 9.7GHz Coaxial CTS Array Results  
Confirmed via FDTD Modeling

- Six-element array

- 19.4 GHz Stubs

- Radius: 22.2 mm
- Width of gap: 5.2 mm
- Positions:
  - Stub 1: 167.7 mm
  - Stub 2: 176.7 mm
  - Stub 3: 185.7 mm

- Gap between sections: 21.9 mm



- 4.2 GHz Stubs

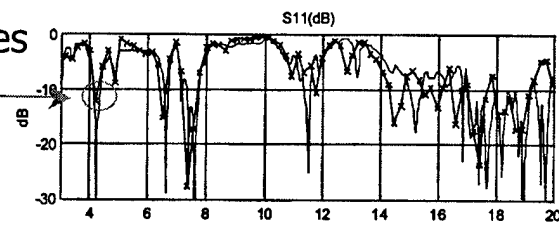
- Radius: 30.6 mm
- Width of gap: 18.9 mm
- Positions:
  - Stub 4: 28.9 mm
  - Stub 5: 77.4 mm
  - Stub 6: 125.9 mm

- Cell Size Used: 0.5 mm  
(scale is in cells)

(a) Multi-Band Coaxial CTS Design

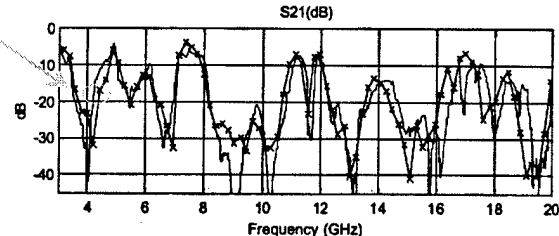
- Previously Simulated Values

- $S_{11} \sim -12$  dB
- $S_{12} \sim -18$  dB



- Our Simulated Values

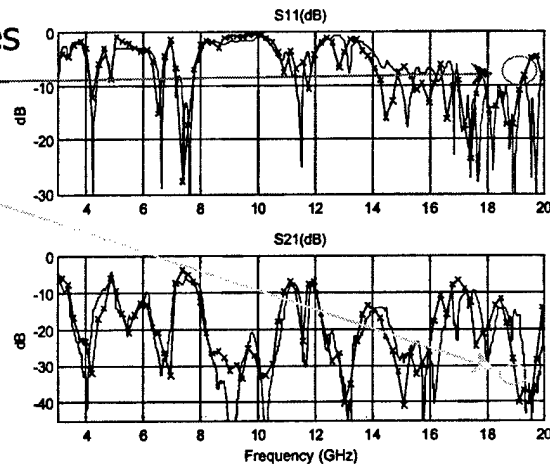
- $S_{11} = -4.8$  dB
- $S_{12} = -7.8$  dB



(b) 4.2GHz Previous & FTFD Results Compared

- Previously Simulated Values

- $S_{11} \sim -4.5$  dB
- $S_{12} \sim -33$  dB



- Our Simulated Values

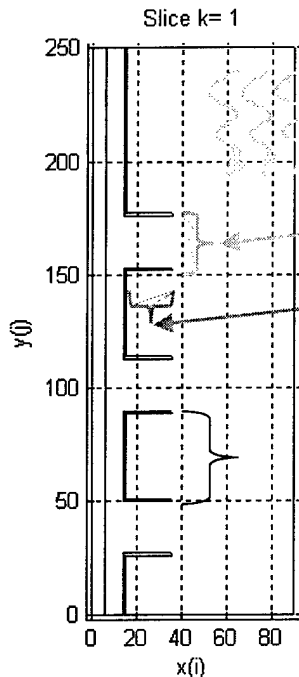
- $S_{11} = -3.6$  dB
- $S_{12} = -24.1$  dB

(c) 19.4GHz Previous & FTFD Results Compared

**Figure 4.1-6.** Previous Multi-Band Coaxial CTS Array Results  
Confirmed via FTFD Modeling

As a first step in this conceptual design task to see if coaxial CTS can be used to address all of the designed bands, the UH team starts by designing and evaluating single band versions for each of the desired bands: 1.8, 2.4, 4.4, 5, 5.7 GHz. The results of this first step are shown in Figures 4.1-7, 4.1-8 and 4.1-9, below.

## 1.8, 2.4, 4.4, 5, 5.7 GHz Arrays



- As Frequency increases:
- Stub Gap Decreases
- Stub Radius Decreases
- Gap Between Stubs Decreases

**Figure 4.1-7.** Single Band Designs First Step Toward Multi-Band Coaxial CTS Arrays

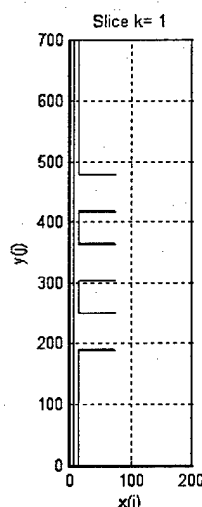
### ■ Stub Parameters:

- Radius: 35 mm
- Width of gap: 30 mm
- Positions:
  - Stub 1: 125 mm
  - Stub 2: 183 mm
  - Stub 3: 243 mm

### ■ Coax Parameters:

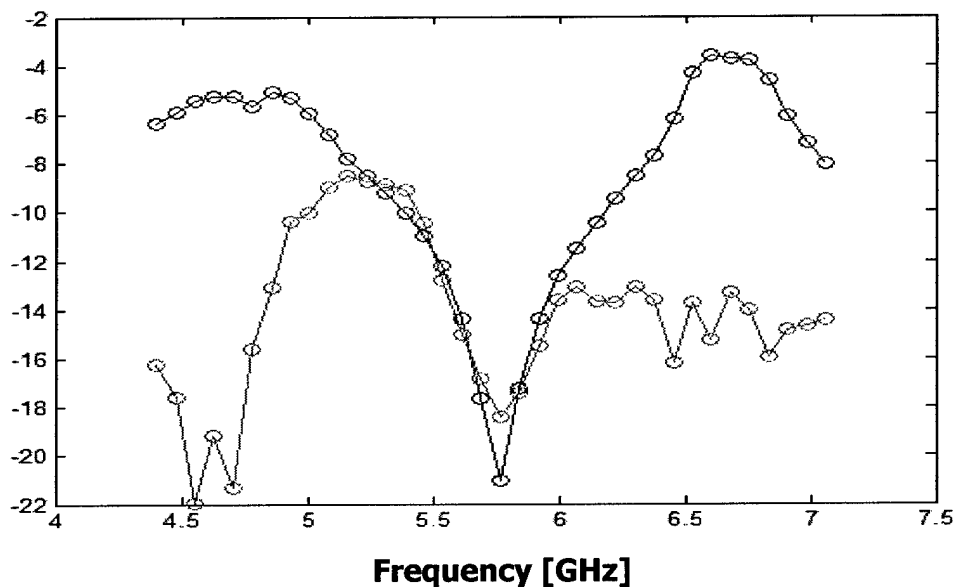
- Inner radius: 3 mm
- Outer radius: 7 mm

### ■ Cell Size Used: 0.5mm



(scale is in cells)

(a) 5.7GHz Coaxial CTS Design



- **S-Parameter Values @ 5.7 GHz**
  - $S_{11} = -21.0115\text{dB}$
  - $S_{12} = -18.4322$

(b) 5.7GHz Simulation Results

**Figure 4.1-8.** Single Band 5.7GHz Design & Results

- **1.8 GHz**
  - $S_{11} = -11.08 \text{ dB}$
  - $S_{12} = -9.22 \text{ dB}$
  
- **2.4 GHz**
  - $S_{11} = -19.06 \text{ dB}$
  - $S_{12} = -11.78 \text{ dB}$
  
- **5.0 GHz**
  - $S_{11} = -12.39 \text{ dB}$
  - $S_{12} = -12.94 \text{ dB}$
  
- **4.4 GHz**
  - $S_{11} = -18.29 \text{ dB}$
  - $S_{12} = -12.80 \text{ dB}$

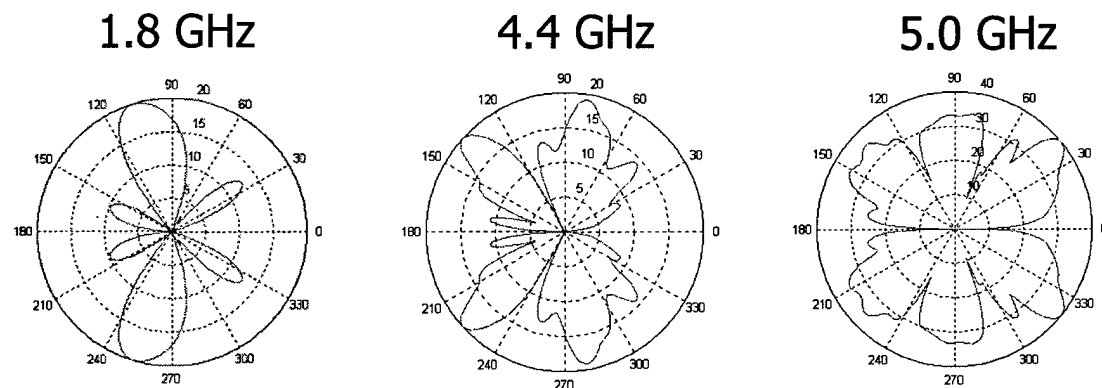


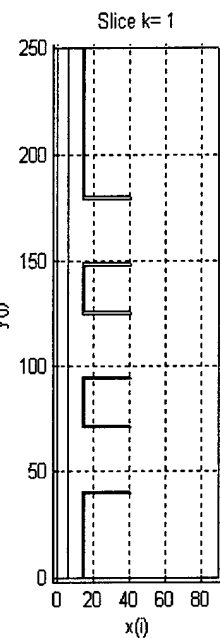
**Figure 4.1-9.** Other Single Band S-Parameter & Pattern Results

The RF design team next collapsed these bands into two separate multi-band arrays (each with three stubs) that each spanned a portion of the bands of interest: 1.8 & 2.5 GHz and 4.4 & 5.9 GHz, and a third 6 stub design spanning 2.4GHz & 5GHz. These arrays shared a common coaxial feed, similar to that shown in Figure 4.1-1. The design of the multi-element arrays was evaluated to assess the feasibility of achieving a single linear array capable of supporting all the bands of interest. The results of this effort are shown in Figures 4.1-10, 4.1-11 and 4.1-12.

- 3-Element Antenna

- Stub Parameters:

- Radius: 60 mm
- Width of gap: 82 mm
- Positions:
  - Stub 1: 142 mm
  - Stub 2: 250 mm
  - Stub 3: 358 mm



- Coax Parameters:

- Inner radius: 12 mm
- Outer radius: 28 mm

- Cell Size Used: 2 mm

(scale is in cells)

- 1.8 GHz

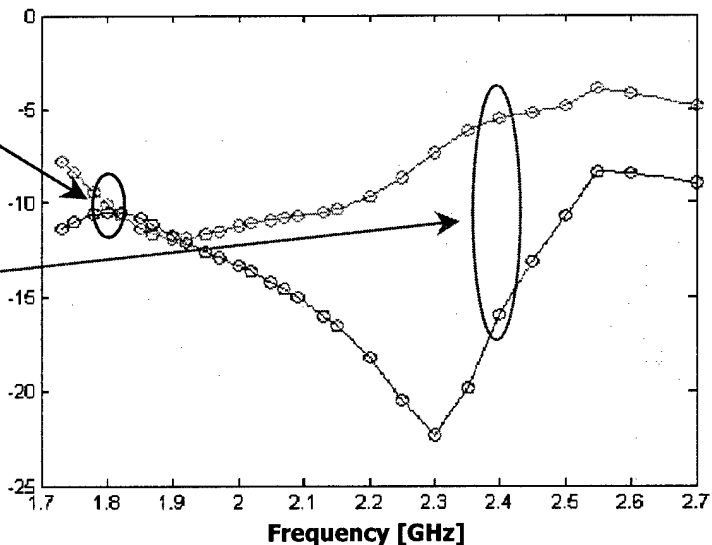
- $S_{11} = 0.29128$   
= -10.47 dB
- $S_{12} = 0.38736$   
= -10.05 dB

- 2.4 GHz

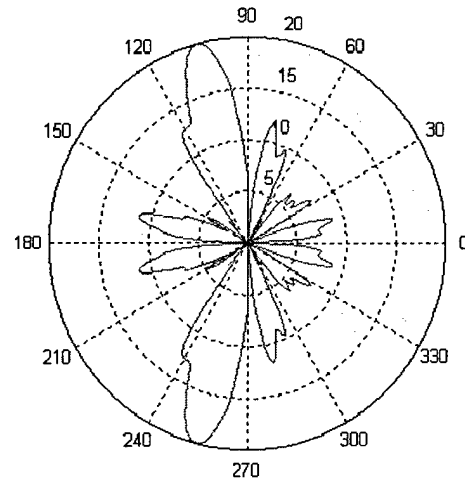
- $S_{11} = 0.24395$   
= -15.974 dB
- $S_{12} = 0.31306$   
= -5.507 dB

- -10 dB bandwidth:

1.8 – 2.25 GHz



1.8 GHz Radiation Pattern



2.4 GHz Radiation Pattern

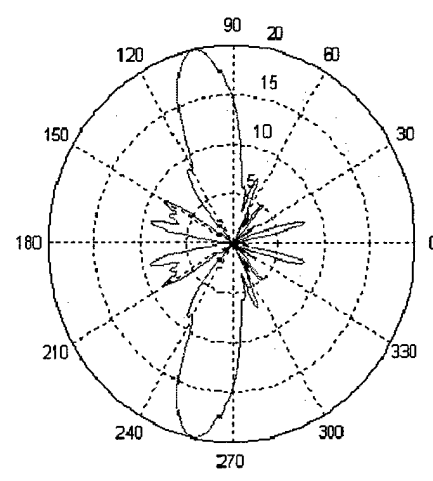
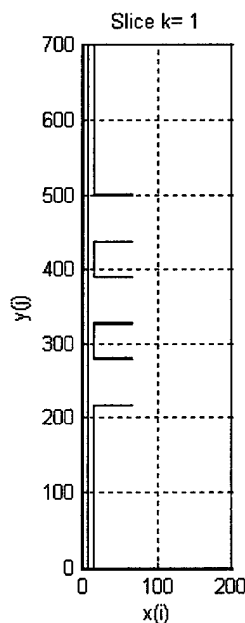


Figure 4.1-10. Multi Band 1.8GHz & 2.4GHz Design & Results

- 3-Element Array

- Stub Parameters:

- Radius: 33.5 mm
- Width of gap: 31 mm
- Positions:
  - Stub 1: 140 mm
  - Stub 2: 195 mm
  - Stub 3: 250 mm



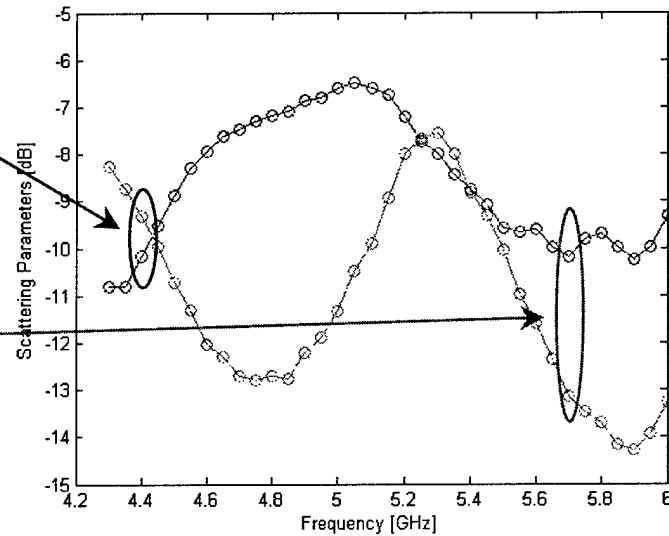
- Coax Parameters:

- Inner radius: 3 mm
- Outer radius: 7 mm

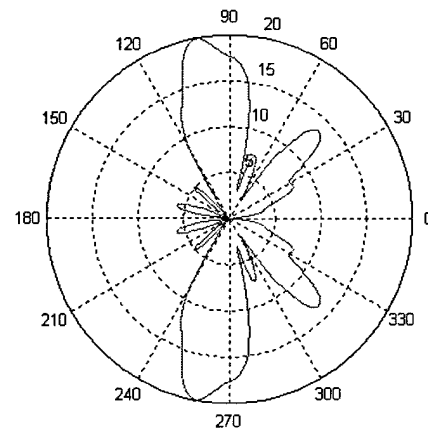
- Cell Size Used: 0.5 mm

(scale is in cells)

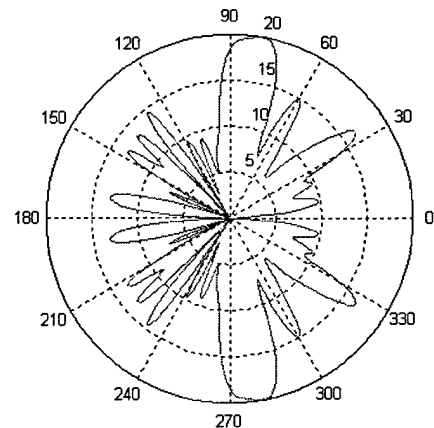
- 4.4 GHz
  - $S_{11} = 0.29128$   
= -10.7137 dB
  - $S_{12} = 0.38736$   
= -8.2377 dB
- 5.7 GHz
  - $S_{11} = 0.24395$   
= -12.254 dB
  - $S_{12} = 0.31306$   
= -10.0873 dB



4.4 GHz Radiation Pattern



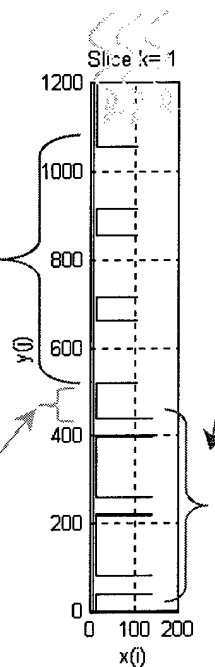
5.7 GHz Radiation Pattern



Both patterns are normalized by 20 dB.

**Figure 4.1-11.** Multi Band 4.4GHz & 5.7GHz Design & Results

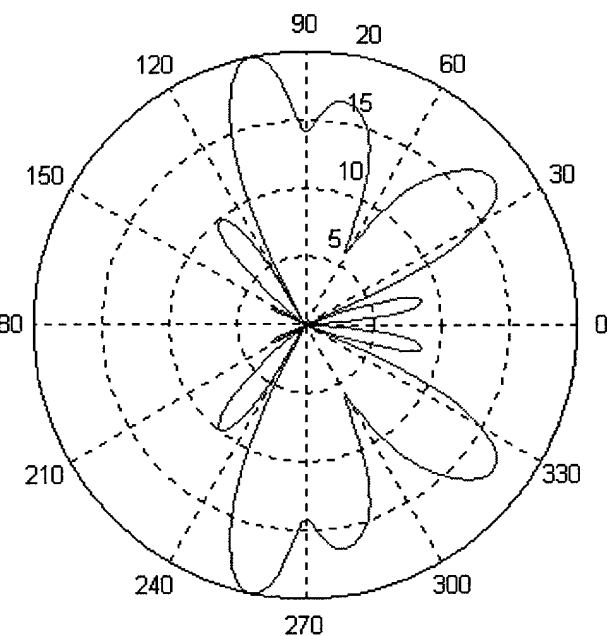
- Two 3-Element Arrays
- 5 GHz Stubs
  - Gap: 70 mm
  - Radius 52 mm
  - Positions:
    - Stub 1: 527.5 mm
    - Stub 2: 427.5 mm
    - Stub 3: 331 mm
- Gap between sections: 41 mm



- 2.4 GHz Stubs
  - Gap: 20 mm
  - Radius: 70 mm
  - Positions:
    - Stub 4: 220 mm
    - Stub 5: 130 mm
    - Stub 6: 40 mm
- Cell Size Used: 0.5 mm  
(scale is in cells)

(a)

- S-Parameter Values
  - $S_{11} = 0.63596$   
= -3.9314 dB
  - $S_{12} = 0.048757$   
= -26.2392 dB
- Radiation Pattern
  - Normalized by 20 dB.



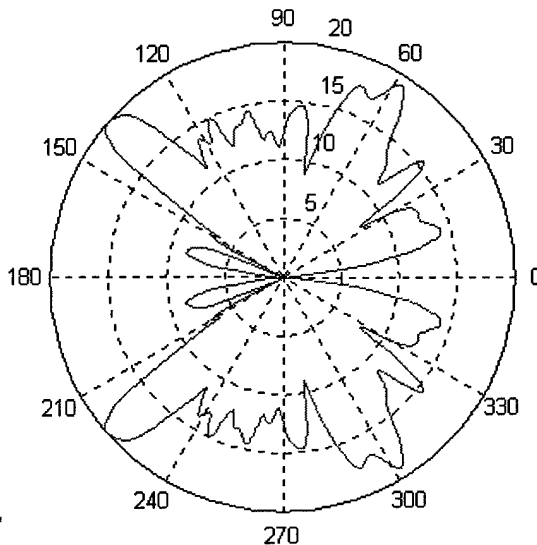
(b) 2.4GHz Results

- S-Parameter Values

- $S_{11} = 0.39626$   
= -8.0403 dB
- $S_{12} = 0.030313$   
= -12.80 dB

- Radiation Pattern

- Normalized by 20 dB.

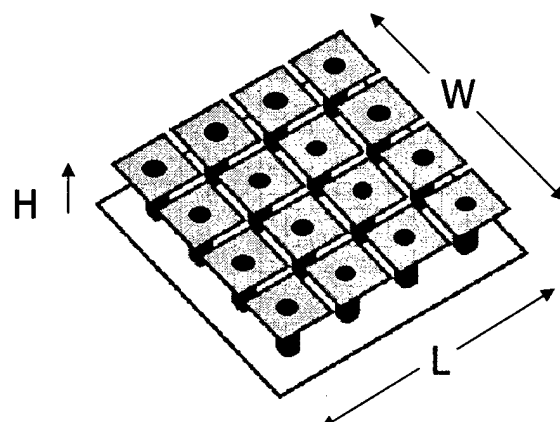


(c) 5.0GHz Results

**Figure 4.1-12. Multi Band 2.4GHz & 5.0GHz Design & Results**

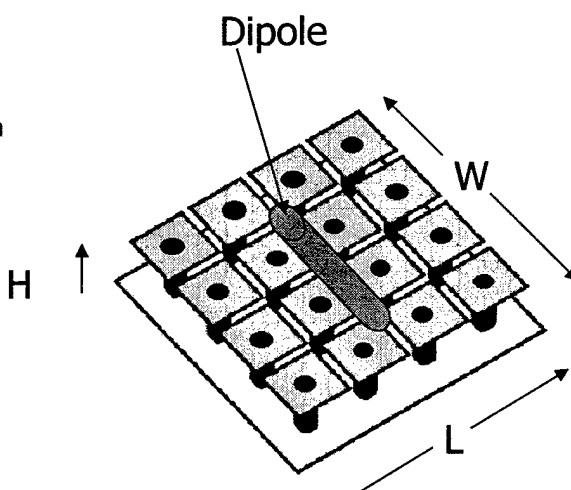
While a subset of the RF design team was working on the Multi-band Antenna discussed above, another subset was focused on a supporting Photonic Band Gap (PBG) structure to serve as a ground plane for the Multi-band Coaxial CTS Antenna and thereby allow the antenna structure to be cut in half (along the coaxial feed plane). The objective of this PBG work is to implement the coaxial CTS designs on the magnetic symmetry plane to provide potential flat mounting while maintaining the omni-directional characteristics, with the hope is that such a PBG structure can be designed to integrate first with individual arrays designed and then with the two multi-band arrays, and thereby to lower the total profile of the Multi-band Antenna. The basic procedure used for the PBG development was to first design magnetic symmetry planes using the PBG structures, and with the support of HFSS, design surfaces at both operating bands, such as 2.4 & 5GHz. Next the individual inductive and capacitive elements of the PBG structures are developed making use of the approximate analytical expressions derived during previous developments of PBG structures. The results of this effort are shown in Figures 4.1-13 and 4.1-14, below.

- $L, W = 93 \text{ mm}$
- $H = 3 \text{ mm}$
- Patch size =  $12.6 \text{ mm} \times 12.6 \text{ mm}$
- Via diameter =  $.36 \text{ mm}$
- Patch spacing =  $.8 \text{ mm}$



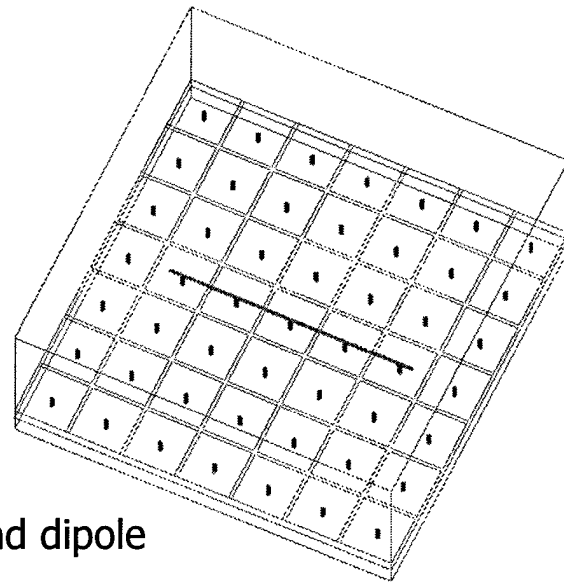
2.4 GHz PBG model

- For testing the characteristics of the developed PBG structure, a dipole antenna was placed on top of the PBG plane and its radiation pattern was calculated
- Dipole tuned to PBG surface resonant frequency
- Dipole placed  $.5 \text{ mm}$  above PBG surface
- Simulations were made for different sizes on the PBG plane, one for  $7 \times 7$  cells, and another for  $9 \times 9$  cells
- The following are the radiation pattern results for both these simulation cases

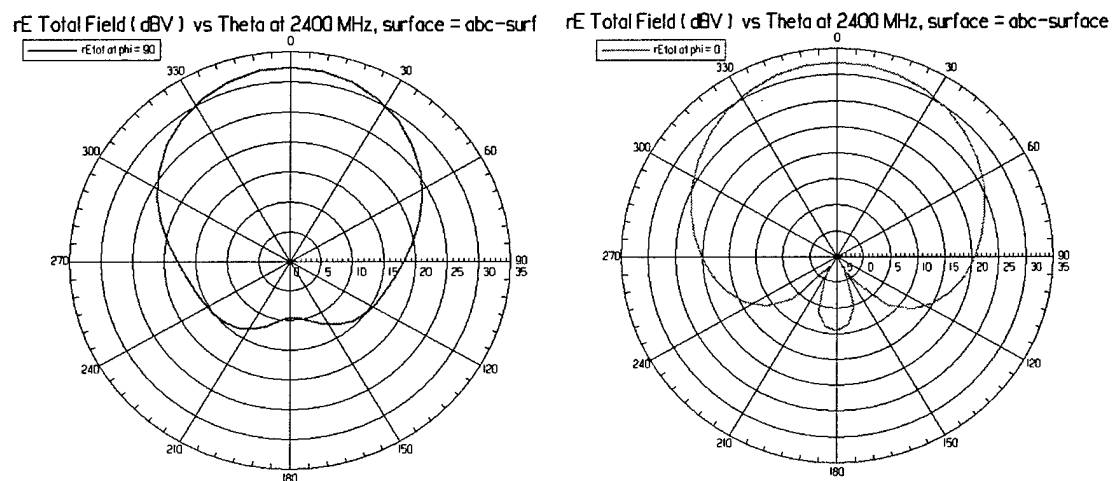


2.4 GHz model and dipole

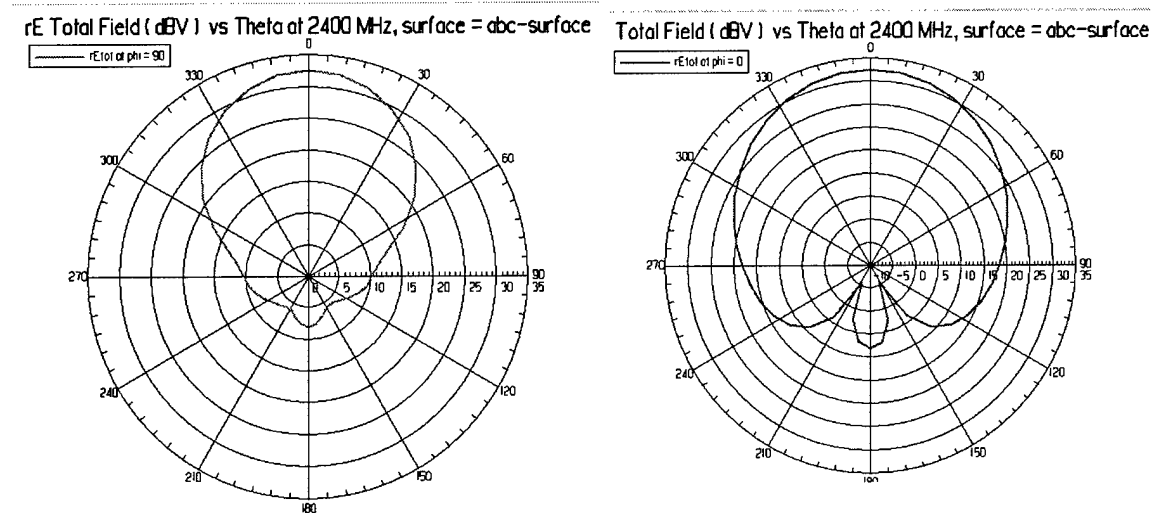
- 7x7 HFSS model
  - 7 rows, 7 columns



HFSS Screen shot of model and dipole



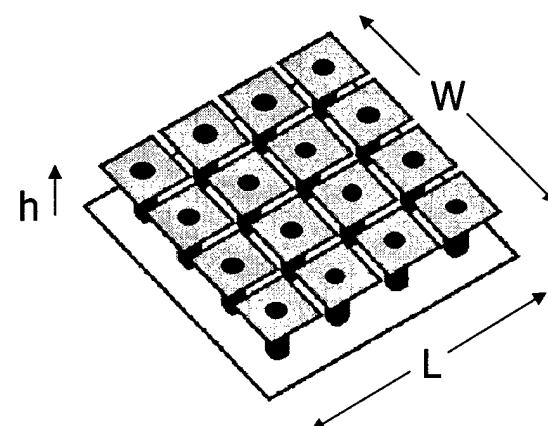
HFSS computed far field radiation patterns of dipole above  
PMC (7x7 cell model). A) YZ plane B) XZ plane



HFSS computed far field radiation patterns of dipole above  
PMC (9x9 cell model). A) YZ plane B) XZ plane

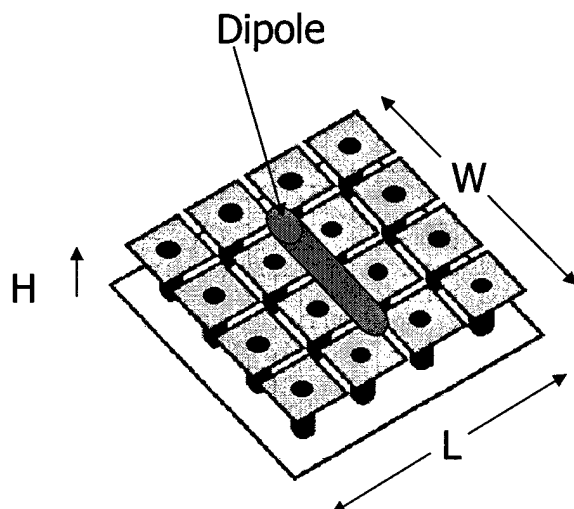
Figure 4.1-13. 2.4GHz PBG Structure Design & Results

- $L, W = 44.4 \text{ mm}$
- $H = 3 \text{ mm}$
- Patch size =  $6 \text{ mm} \times 6 \text{ mm}$
- Via diameter =  $.36 \text{ mm}$
- Patch spacing =  $.4 \text{ mm}$



5 GHz model

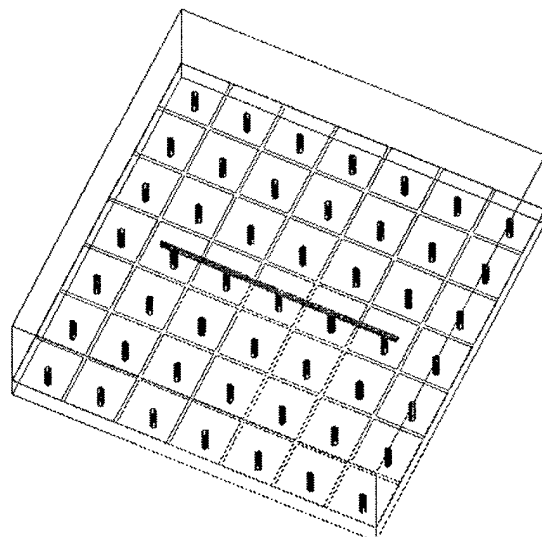
- Dipole tuned to PBG surface resonant frequency (5 GHz)
- Dipole placed .5 mm above PBG surface

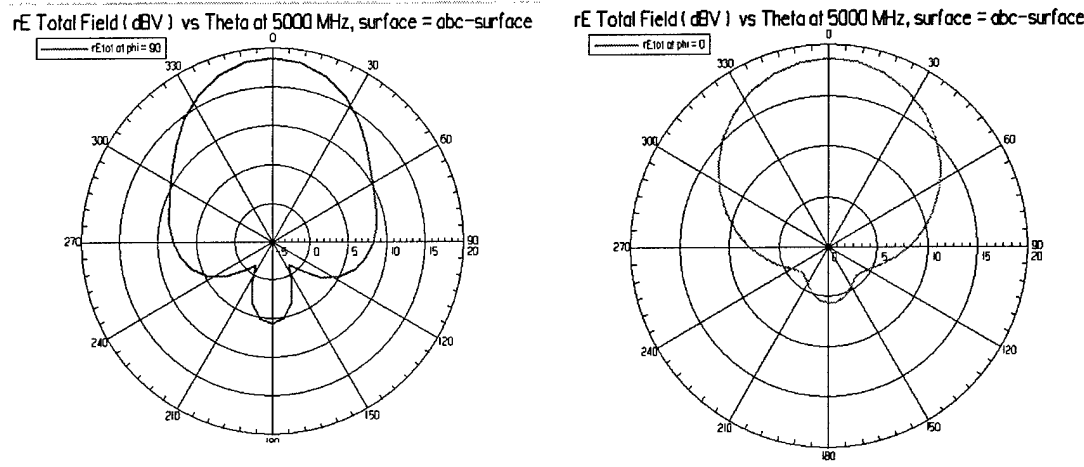


5 GHz model and dipole

- 7x7 model
  - 7 rows, 7 columns

HFSS Screen shot of model and dipole





HFSS computed far field radiation patterns of dipole above PMC (7x7 cell model). A) YZ plane B) XZ plane

**Figure 4.1-14. 5GHz PBG Structure Design & Results**

#### 4.2 Wideband WAVETRAP Antenna

The following figures briefly illustrate the analysis/design process that is currently being employed in the Phase I design. Starting with the canonical case of a single stub radiating into an open half-space, the field components are analyzed and optimized employing the Finite Element Method (FEM). This method allows for the accurate simulation (visualization) of both field components and far-field patterns as illustrated below:

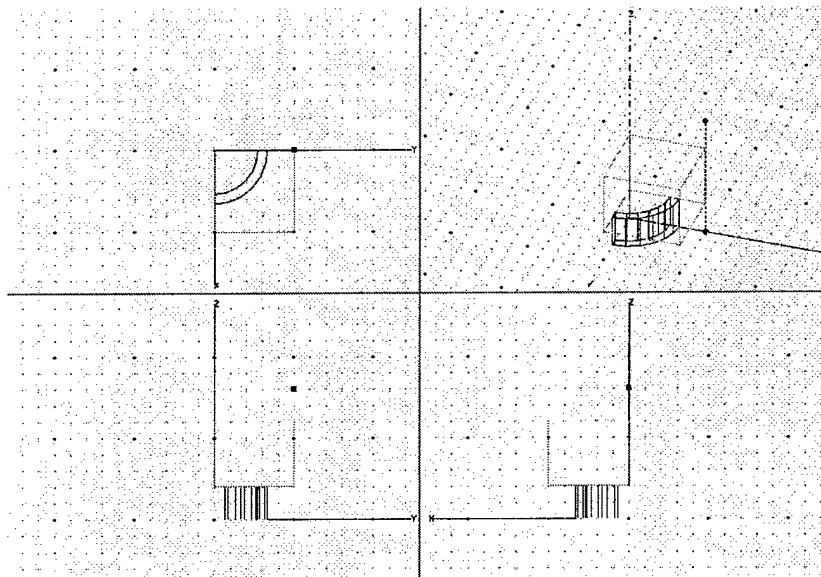


**Figure 4.2-1: Single Isolated Annular Radiating Stub (Two-Plane Symmetry)**

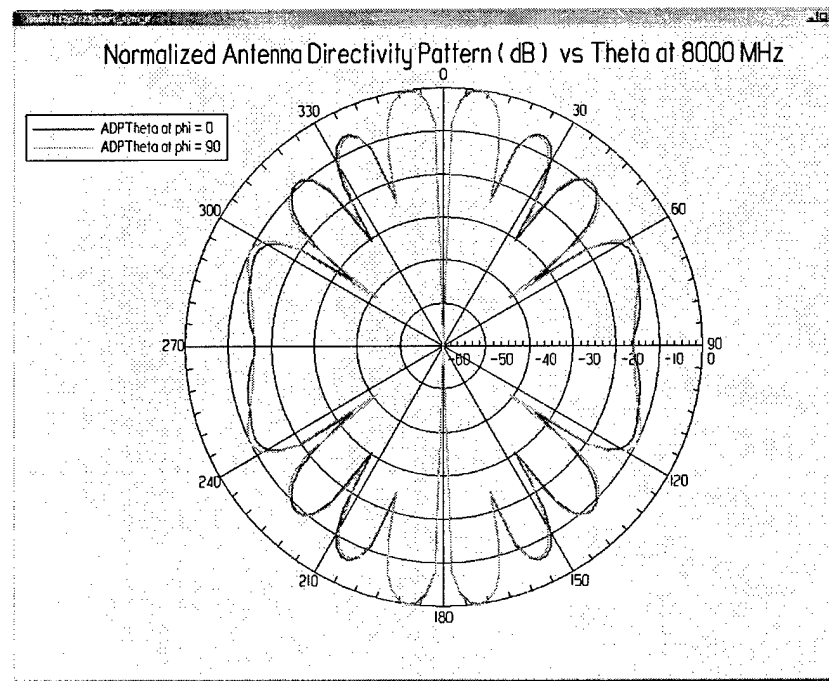


**Figure 4.2-2: Computed Elevation-Plane Pattern for Single Isolated Annular Stub (8000 MHz)**

Based on the canonical (single) stub results, multiple radiating stubs are introduced and analyzed in order to assess and exploit mutual coupling as well their self-impedance (active impedance) characteristics in the presence of multiple stubs in the conducting ground-plane.

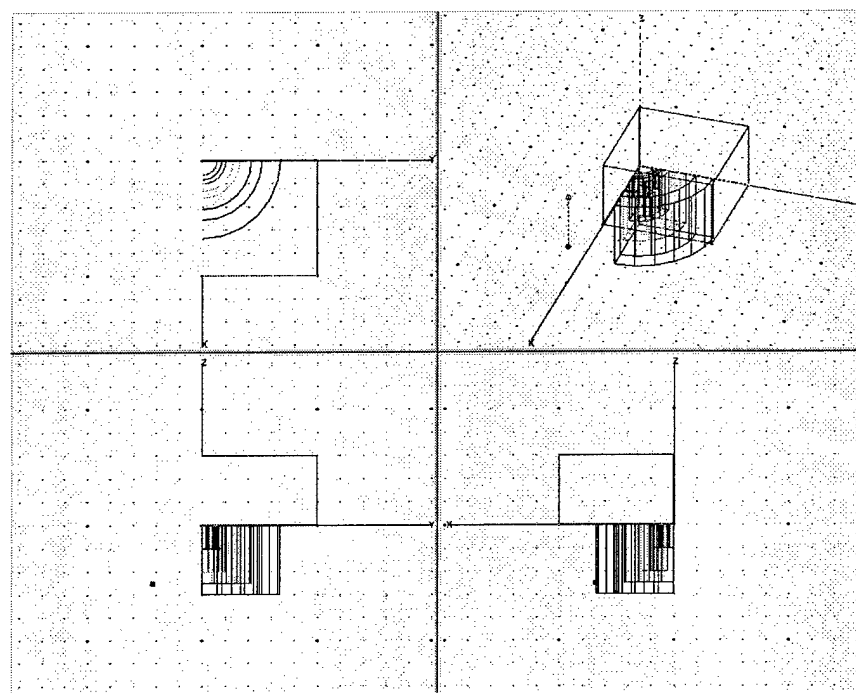


**Figure 4.2-3: Multiple Radiating Annular Stubs (Two-Plane Symmetry)**

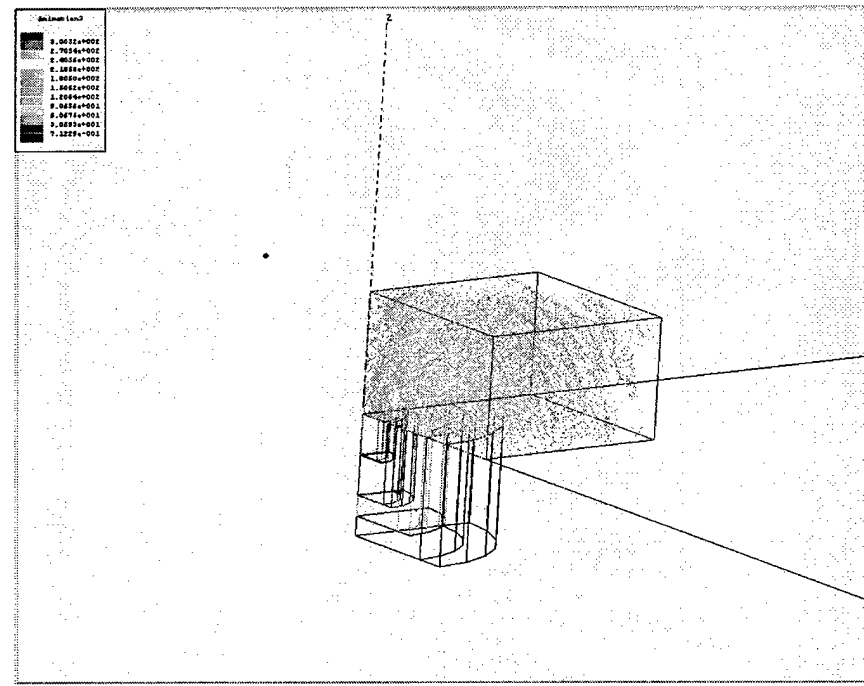


**Figure 4.2-4: Computed Near-Field Intensities for a Representative Embedded Radiating Annular Stub**

These active impedance (complex reflection coefficients) are currently being used in order to determine the optimal phase and amplitude relationships (as set and directly

driven by the radial waveguide-based corporate feed network) that result in an optimal input match over the bandwidth of interest (VSWR < 2.0:1)

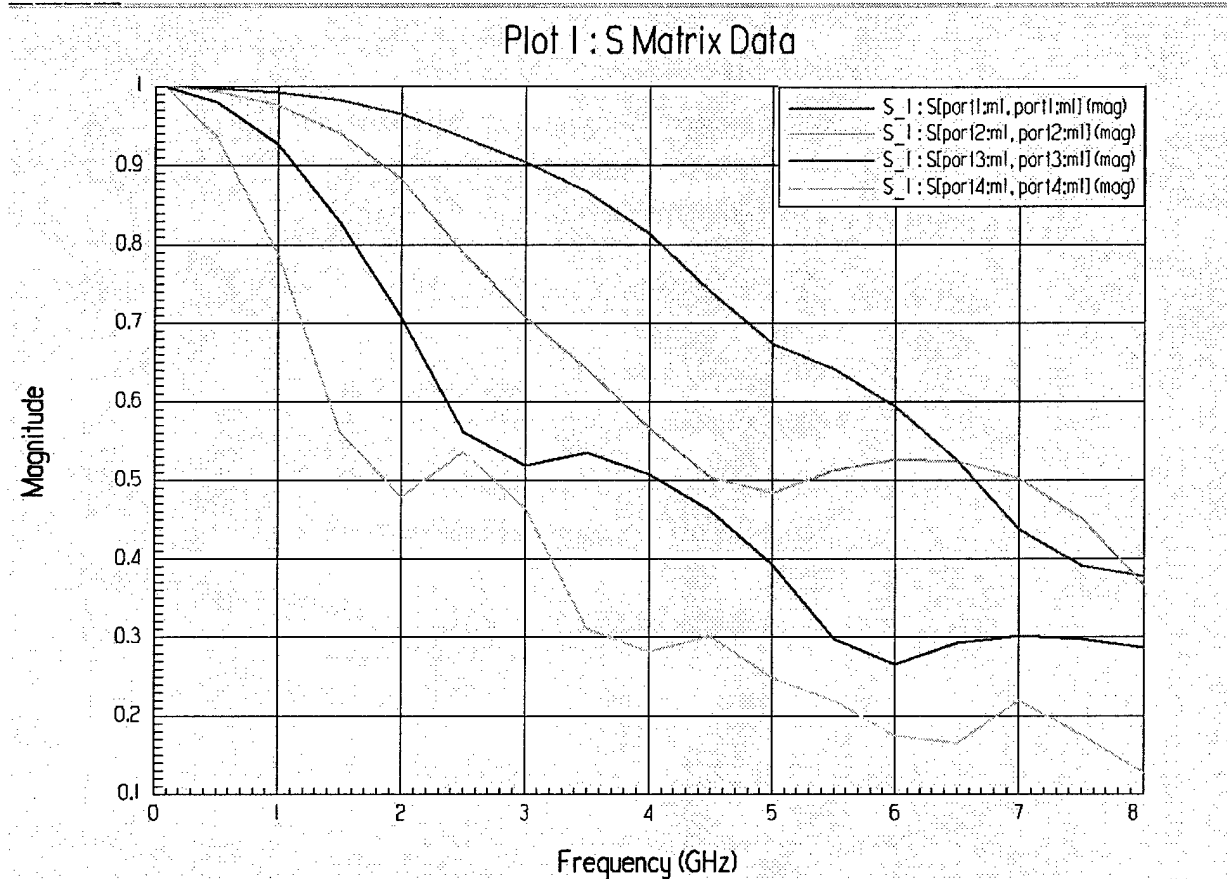


**Figure 4.2-5: Active Reflection Coefficient Magnitudes for Concentric Annular Radiating Stubs**

An SMA coaxial connector interface is currently baselined for this design. Similar to the radiating aperture and radial-waveguide transmission-line sections, the input is similarly modeled using the Finite Element Method (FEM).

Based on the anticipated notional operational battlefield profile and the desired coverage range (minimum and maximum), an idealized beamshape is synthesized in order to provide the desired footprint and specified ripple. A conjugate-phase synthesis technique (adapted to cylindrical coordinates) is then used to compute the idealized excitation amplitude and phase for each annular stub. Larger diameter arrays enable better conformance (lower ripple) realizations of the ideal beamshape at the expense of greater weight. This particular synthesis technique (and trade) is relevant to the WAVETRAP designs and several different size/performance options and results will be presented in our final report.

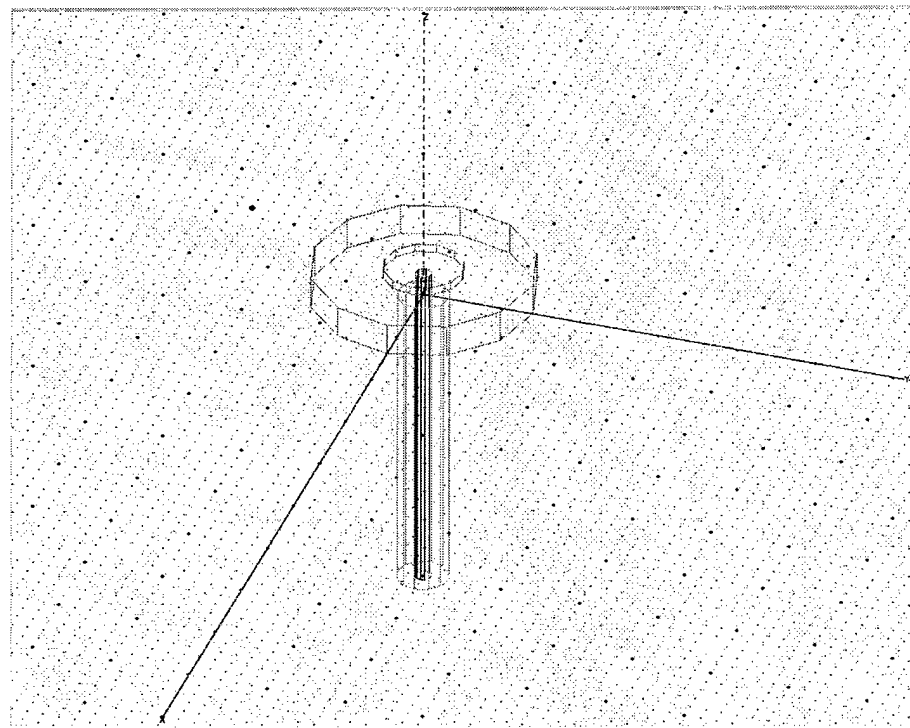


**Figure 4.2-6: Coaxial Connector Interface Geometry**

In addition to the above investigations of the radiating aperture structure and interface characteristics, ThinKom initiated investigations into the impact of finite ground planes around the radiating aperture performance and pattern characteristics as well as the necessary analysis tools to conduct these investigations. Starting with a basic model for a monopole antenna (since WAVETRAP offers a low profile equivalent of a monopole) we used our analysis tools to generate the proportional impacts of finite ground plane size on antenna gain, amplitude and angle of maximum gain:

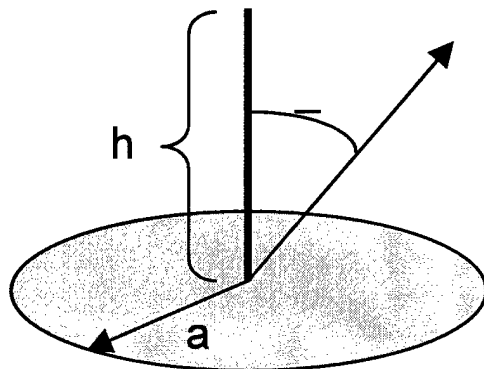


**Figure 4.2-7: Generic Isolated Monopole Model for Assessment of Finite Groundplane Effects**

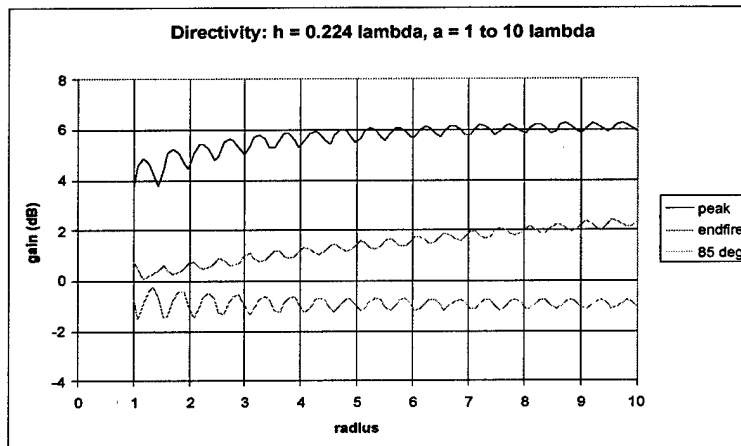


**Figure 4.2-8: Peak and On-Horizon Monopole Gain vs. Finite Groundplane Radius (in Wavelengths)**

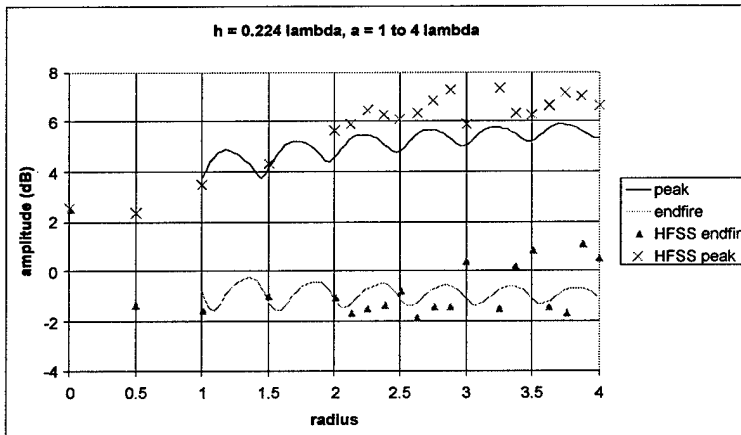


**Figure 4.2-9: Peak and On-Horizon Monopole Gain vs. GP Radius (Exp. Scale, FEM and GTD Codes)**

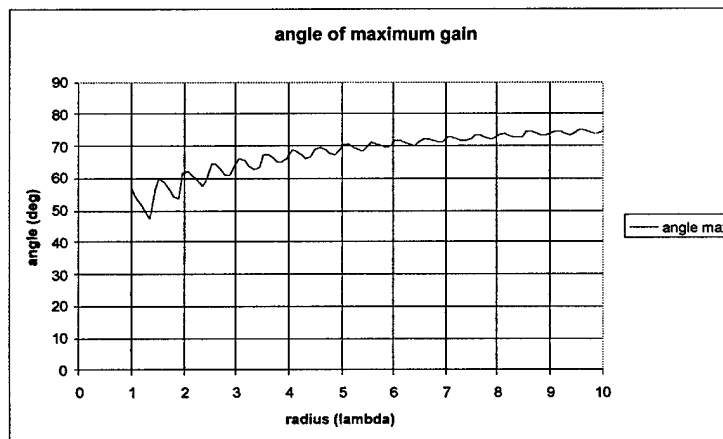


**Figure 4.2-10: Elevation Angle of Monopole Gain Maximum vs. GP Radius**

We observed that the angle of peak radiation and the relative gain decreases with decreasing ground plane size. This indicates that “Finite” Groundplane effects are fundamental to on-horizon performance even for “large” (10 Lambda Radius or Larger) groundplanes and installations. By modeling the monopole in the presence of a finite ground plane using HFSS (High Frequency Structural Simulation) we were able to quantify the departure of the resultant radiating patterns from those that would be expected in the “traditional” infinite groundplane environment. In addition, we employed a (more numerically efficient) code based on the Uniform Theory of Diffraction (UTD) as a comparative check to these results. Most noteworthy of these finite effects is the unfavorable “lifting” of the antenna gain peak above the horizon for all but the largest groundplanes, thereby reducing gain along the horizon (where slant ranges and gain requirements are generally highest.) The WAVETRAP effectively addresses this issue by directly driving the surface currents in a prescribed controlled manner, rather than depending on the parasitically-induced currents associated with a typical monopole installation.

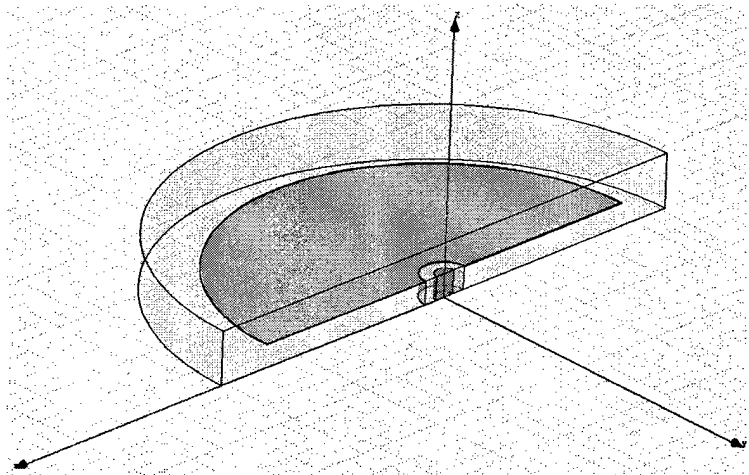


**Figure 4.2-11: Geometry for Canonical Annular Radiating Stub in the Presence of a Finite Groundplane**

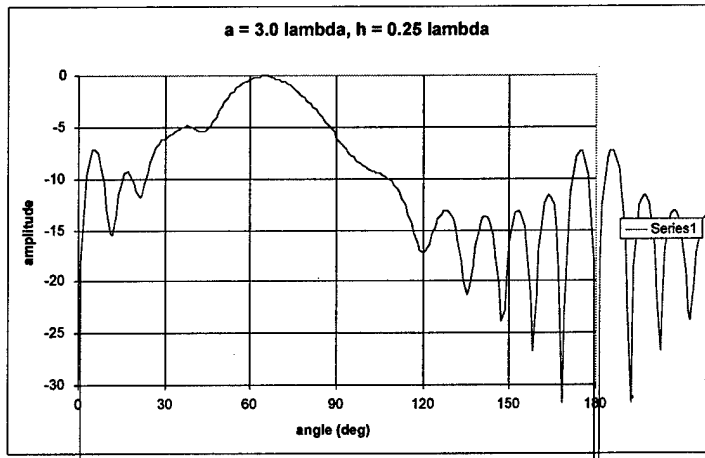


**Figure 4.2-12: Elevation Plane Pattern for Monopole over Finite Groundplane ( $R_{gp} = 3 \text{ Lambda}$ )**

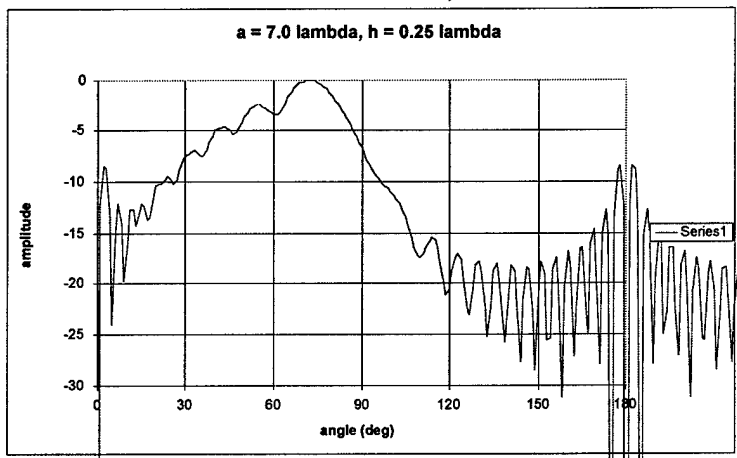


**Figure 4.2-13: Elevation Plane Pattern for Monopole over Finite Groundplane ( $R_{gp} = 7 \text{ Lambda}$ )**

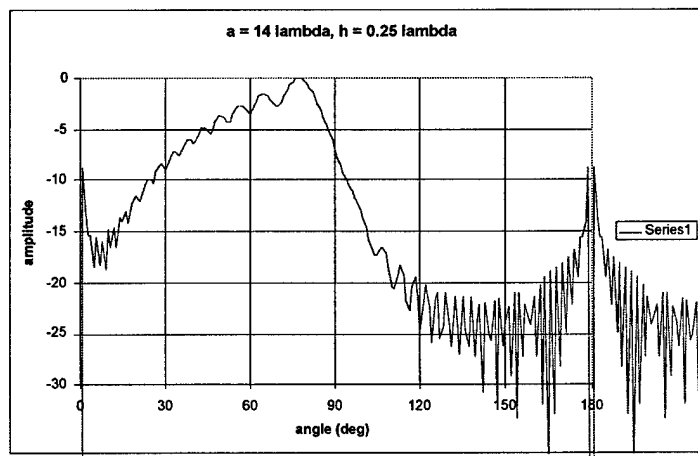


**Figure 4.2-14: Elevation Plane Pattern for Monopole over Finite Groundplane ( $R_{gp} = 14 \text{ Lambda}$ )**

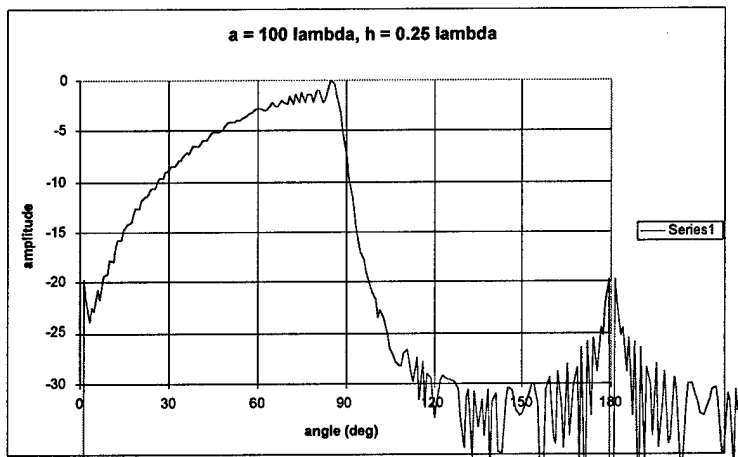


**Figure 4.2-15: Elevation Plane Pattern for Monopole over Finite Groundplane  
( $R_{gp} = 100$  Lambda)**

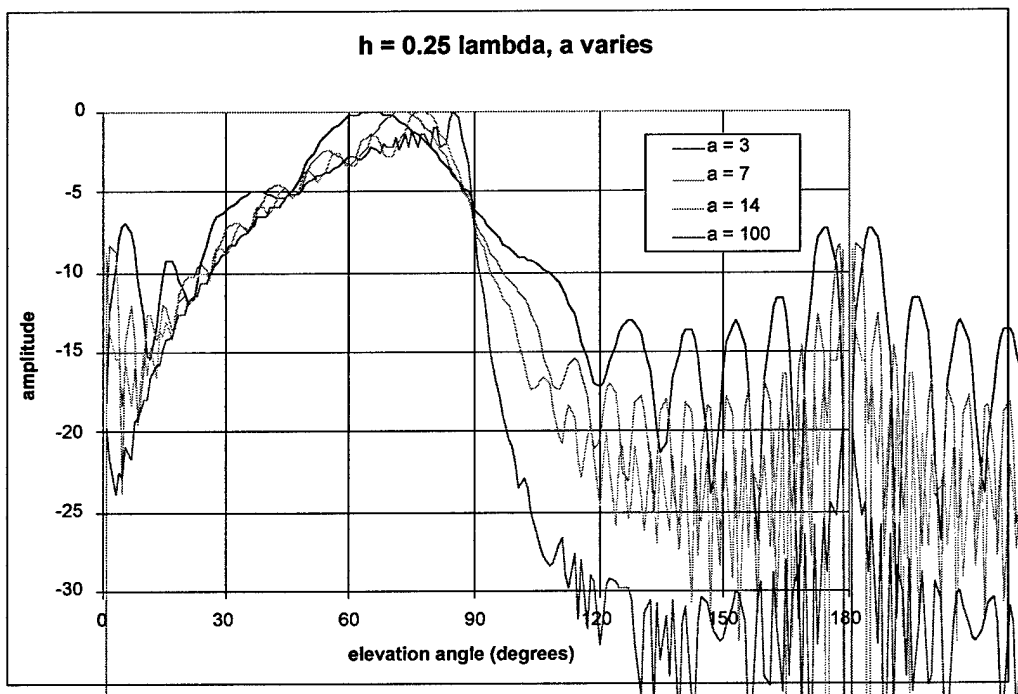


**Figure 4.2-16: Elevation Plane Patterns for Monopole over Finite GP ( $R_{gp} = 3, 7, 14, 100$  Lambda)**

These design analysis and installed performance tools can be used to project the RF and installed performance of the prototypes in Phase II, and thereby validate such predictions making use of the AFRL measured test results.

## **5. Project Summary and Follow-on Recommendations:**

The conceptual development work completed by the University of Hawaii in support of ThinKom on this project successfully showed the capability of the coaxial CTS antenna technology multiple bands fed by a single coaxial line, and spanning all the bands of interest for this SBIR topic. In fact these multi-band coaxial CTS antennas also showed significant gain increase (upwards of 20dB), however, the antenna patterns showed two main lobes within the full spherical region. This characteristic of coaxial CTS can be dealt with by mounting half of the circular coaxial stub above a broadband ground plane that would focus all the radiated energy into a single hemispherical region. The PBG investigations showed that such could be achieved using that technology for the individual bands, but had not shown it could be achieved for multiple bands. However, past research with PBG ground planes have shown the capability to support multiple bands similar to those of interest for this project. The next two steps in this line of research would be to; 1) complete the demonstration of a single PBG ground plane supporting at least two bands (the same bands) as were shown for the multi-band coaxial CTS arrays plus to build such a ground plane to support a demonstration with a coaxial CTS array, and 2) construct a multi-band coaxial CTS array (at least a dual band array as analyzed and simulated during this investigation) in which the stubs are only half circles and then to mount this coaxial CTS array above the PBG ground plane, and the assembly used to show the achieved patterns. While the latter half of these needed steps (the detailed design and fabrication of the demonstration prototype antenna, and testing thereof) was intended to be part of the Phase II effort, it was intended when Phase I was started that all the conceptual development would be completed with Phase I, however, it turned out that insufficient time and resources were available to complete this conceptual development to the point where all the needed building blocks had been sufficiently investigated to support even a crude preliminary design of said prototype. It should also be noted that no effort was applied (nor proposed to be applied) to a rather critical element of the final antenna system architecture, the phase shifters needed to steer the coaxial CTS beam in either the elevation or more importantly the azimuth plane. Admittedly the multi-band coaxial CTS array and the PBG ground plane were the needed first steps, however, at least conceptual research will be needed to define a satisfactory approach and the basic requirements for such steering, whether static (e.g. for elevation) and/or dynamic (e.g. for azimuth). In summary the coaxial CTS array approach still appears suitable for the desired application (a multi-band array in the lower bands), however, much more research is needed to confirm the reasonably expected performance and reasonable methods to be used for detailed design and fabrication of even the initial prototype antenna array, much less the eventual antenna array(s) for operational use.

In parallel with the University of Hawaii investigation of the coaxial CTS approach to providing a high gain antenna in support of the desired multi-band mobile wireless local area network (LAN or WLAN), ThinKom has been investigating our previously invented WAVETRAP antenna technology as another possible antenna solution to the multi-band mobile WLAN requirements. We have included some of the results from our investigation of the most obvious difference between the coaxial CTS and WAVETRAP; WAVETRAP is a naturally broadband antenna technology that can span the entire

desired set of bands in a single antenna structure. We have shown that it is possible to span the bandwidth in a single broad beam antenna and have carried those investigations into considering the surrounding natural (i.e. the metal roof of a ground vehicle) ground plane and how that impacts the performance of this very broadband antenna. Again, due to the fact that we ran out of time and resources to apply to this investigation we did not carry the definition of WAVETRAP modes of from the broad beam (near omni-directional mode) to include the directional mode of operation. In this mode we can feed individually the azimuth segments, formed by the feed design, and each of these segments can separately form a beam of increased gain (about 10-12dBi) relative to the omni-directional mode (about 4dBi) gain. If added gain is desired we would need to trade off two approaches: 1) increase the size of the antenna diameter, or 2) attempt to phase combine several co-located antennas. The azimuth steering of the beam is easily handled by simply switching between the various feed points of the azimuth segments.

ThinKom will be continuing the investigations into the WAVETRAP antenna technology, and we are moving toward our initial commercial product which is intended to cover nearly the same as the desired bands for the SBIR topic: from below 2GHz to 6GHz. After the completion of those investigations and fabrication and test (in the omni-directional mode of operation) of that prototype, our internally funded development plans will include the investigation of the directional mode of operation for WAVETRAP. ThinKom's interest in the directional mode of operation is for applications in the commercial automobile marketplace, including the investigation of mobile WLAN between ground vehicles in a commercial setting such as between emergency vehicles and consumer cars. If there is continued interest by the US Army in the WAVETRAP antenna technology, please let us know (by the way, we were selected for a Air Force SBIR seeking JTRS solutions for aircraft and WAVETRAP is the primary focus).